

Sensitivity of quantum walks to a boundary of two-dimensional lattices: approaches from the CGMV method and topological phases

Takako Endo,¹ Norio Konno,² Hideaki Obuse,³ Etsuo Segawa.⁴ *

¹ Institute for Global Leadership, Ochanomizu University

2-1-1 Ohtsuka, Bunkyo, Tokyo, 112-0012, Japan

² Department of Applied Mathematics, Faculty of Engineering, Yokohama National University

Hodogaya, Yokohama 240-8501, Japan

³ Department of Applied Physics, Hokkaido University

Sapporo, Hokkaido 060-8628, Japan

⁴ Graduate School of Information Sciences, Tohoku University,

Aoba, Sendai 980-8579, Japan

Abstract. In this paper, we treat quantum walks on the two-dimensional lattice with the cutting edge at $x = 0$ introduced by Asboth and Edge [Phys. Rev. A **91**, 022324 (2014)] in order to study one-dimensional edge states originating from topological phases and to see a collateral evidence how a quantum walker reacts such a graph deformation making the boundary. Firstly, we connect this model to the CMV matrix which provides the 5-term recursion relation of the Laurent polynomial associated with spectral measure on the unit circle. Secondly, we obtain the dispersion relation of the energy of the quantum walk explicitly by using the spectral analysis of the CMV matrix. We confirm that the dispersion relation for edge states are consistent with the prediction from the topological phases originating from not only two-dimensional bulk states but also one-dimensional ones in a certain condition. Finally, we show how the edge states contribute the asymptotic behavior of the quantum walk through limit theorems of the finding probability. Conversely, we also propose a differential equation using this limit distribution whose solution is the underlying edge state.

1 Introduction

Quantum walks were introduced by quantum analogue of random walks [14]. The first trigger of intensively tackling quantum walks came from the field of quantum information [1]. Nowadays, overlaps between quantum walks and not only quantum information but also various research fields have been found and established interdisciplinary researches, see [20, 23] and its references therein.

*e-segawa@m.tohoku.ac.jp

Key words and phrases. quantum walks, topological phase, CMV matrix

One of the recent novel stream of the study on quantum walks is connecting quantum walks to topological insulators. Kitagawa *et al.* [15, 16] introduced a quantum walk model as a topological insulator model lattice which is simplified by temporal and spatial discretization. In particular, quantum walks on the one-dimensional lattice, whose unitary time evolution retains chiral symmetry and is spatially inhomogeneous have been intensively studied e.g., [2, 8, 9, 10, 11, 22, 21]. Kitagawa[16] also introduced the connection between two-dimensional topological insulators and quantum walk models on a two dimensional square lattice[12, 13]. Asboth and Edge provided further studies on this model with the “cutting edge” [4]. Here the “cutting edges” is that we cut all the edges of \mathbb{Z}^2 between $(0, y) \in \mathbb{Z}^2$ and $(-1, y) \in \mathbb{Z}^2$ for $y \in \mathbb{Z}$ and rewire these edges as the self loop on $(0, y)$. This model is determined by a pair of two parameter $(\alpha, \beta) \in [0, 2\pi)^2$: the first and second parameters α and β determine a local dynamics of the horizontal and vertical directions on the two-dimensional lattice, respectively. The local dynamics is provided by acting the two-dimensional α and β rotation matrices to the two-dimensional internal state, alternatively. See for the detailed definition of this graph setting and the time evolution in Section 2. Asboth and Edge provided some analytical and numerical results on the existence of unidirectional edge states along self loops. We call this model the AE model. In this paper, we provide further analytical results on the AE model. The main purpose of this paper is to close the answer of the following question throughout the AE model: after getting the measurement value of the quantum system iterated by the unitary time evolution as the “distribution”, how can we estimate the underlying spectral construction of the unitary time evolution operator?

To this end, firstly, we connect the AE model to the CMV matrix (Theorem 1). Due to the translation symmetry with respect to the vertical direction of the AE model, we can take the Fourier transform and decompose the time operator U into the unitary operators $\{\hat{U}(k)\}_{k \in [0, 2\pi)}$. Interestingly, we find that $\hat{U}(k)$ for each k is isomorphic to the CMV matrix with null-odd Verblunsky parameter

$$(\eta(k), 0, \eta(k), 0, \dots), \quad \eta(k) = \sin(\alpha - \beta) \cos k + i \sin(\alpha + \beta) \sin k.$$

Thanks to this connection, secondly, we can describe explicitly the dispersion relation, which provides the relation between wave number $k \in [0, 2\pi)$ and the quasi-energy $\theta \in [0, 2\pi)$, that is, we obtain two bulks with the gap $Bu \in [0, 2\pi)^2$ and the edge state $Ed \in [0, 2\pi)^2$ between the two bulk. (Theorem 2) As a corollary, we can classify the dispersion relation into the signs of

$$(\text{sgn}(\sin 2\alpha \sin 2\beta), \text{sgn}(\sin(\alpha + \beta)), \text{sgn}(\sin(\alpha - \beta))).$$

We also introduce topological phases studied in Ref. [4] and derive topological phases reflecting one-dimensional nature. We argue the relation between the dispersion relation derived from Theorem 2 and topological phases in figures 2–10.

Thirdly, we examine how the quantum walk feels the boundary on the two dimensional case (Theorem 3). On the one-dimensional lattice, if the edge state exists, then we observe localization, that is, the time averaged limit measure is strictly positive, as the stochastic phenomena of the quantum walk [10, 22]. To express the response of the quantum walk on the boundary for two-dimensional case, we define $\nu_n : \partial D \rightarrow [0, 1]$ so that $\nu_n(j)$ is the finding probability of the AE model at the n -th iteration and at the self loop on $[0, j] \in \mathbb{Z}_+ \times \mathbb{Z}$ starting from the self loop at the origin. We show that the response is classified into the four behaviors up to the parameter (α, β) :

- (1) continuously-linear spreading
- (2) ballistic spreading
- (3) localization
- (4) null

In particular, the limit density function of (2) is described by using the Konno distribution [17, 18]. The limit behavior of the quantum walk contributed by the edge state in the case of (2) is completely expressed in Theorem 4.

As a consequence, putting the group-velocity $v(k)$, quasi-effective mass $M(k)$ and the density of the edge state $m_0(k)$, we obtain a parametric plot of the limit density function of (2) by using these physical quantities (see Corollary 3.) By this parametric plot expression, conversely, we can take an estimation of the underlying edge state from the obtained distribution. More precisely, if we can get some estimation \tilde{g} of the true limit distribution g from a data of the distribution obtained by the measurement of self loops after the unitary time finite iterations, then the underlying edge state can be also estimated from this data by solving the following differential equation with some constant $c \in \mathbb{R}$; $\tilde{g}(v) dv/dk = cv^2$, which implies that the group velocity of edge state is an inverse of the Konno distribution in this model (see Corollary 4).

This paper is organized as follows. In Sect. 2, we define the graph and the quantum walk treated here. In Sect. 3, we connect the quantum walk with the CMV matrix. Section 4 is devoted to the spectral analysis and the dispersion relation in addition to topological phases of the AE model. In Sect. 5, we present how the property of the spectrum obtained in the previous section is reflected to the stochastic behavior along the boundary by studying limit distribution functions. Finally, in Sect. 6, we present limit distribution functions towards bulk, which clearly exhibits exponential decays.

2 Model

2.1 Graph

Let $G = (V, A)$ be a directed graph whose vertex set and arc set are V and A . In this paper, we set the vertex set by

$$V = \mathbb{Z}_+ \times \mathbb{Z} = \{(x, y) \mid x \in \mathbb{Z}_+, y \in \mathbb{Z}\},$$

where \mathbb{Z} is the integer set and \mathbb{Z}_+ is the non-negative integer set. We denote the boundary of this graph by $\partial D := \{(0, j) \in V : j \in \mathbb{Z}\}$. For $a \in A$, the origin and terminus of a is denoted by $o(a), t(a) \in V$, and the inverse of a is denoted by \bar{a} . The arcset A is represented by

$$A = \{(\mathbf{x}; d) \mid \mathbf{x} \in V, d \in \{0, 1, 2, 3\}\}.$$

Here if $a = (\mathbf{x}; d) \in A$, then

$$t(a) = \mathbf{x},$$

$$o(a) = \begin{cases} \mathbf{x} + (1, 0) & : d = 0, \\ \mathbf{x} & : d = 1, \mathbf{x} \in \partial D, \\ \mathbf{x} - (1, 0) & : d = 1, \mathbf{x} \notin \partial D, \\ \mathbf{x} + (0, 1) & : d = 2, \\ \mathbf{x} - (0, 1) & : d = 3, \end{cases}$$

which means that $(\mathbf{x}; d)$ is the arc coming from the direction d whose terminus is \mathbf{x} . See figure 1. We call $\{(\mathbf{x}; 1) \mid \mathbf{x} \in \partial D\} \subset A$ a set of self loops. We take $\bar{a} = a$ for every self loop.

2.2 Definition of AE model

The one step time evolution of AE model is that the incident state coming from the horizontal (vertical) direction is transmitted at the terminal vertex to the vertical (horizontal) directions with some complex valued weight conserving the unitarity. Here, we define the model for a Hilbert space $\ell^2(A)$ in the arc set representation at first, then convert it to one in the vertex sets $\ell^2(V; \mathbb{C}^4)$ or $\ell^2(V; \mathbb{C}^2)$ representations.

- (1) Total Hilbert space: $\mathcal{A} := \ell^2(A) = \{\psi : A \rightarrow \mathbb{C} \mid \|\psi\| < \infty\}$. The inner product is the standard inner product. Now we introduce a binary relation of A .

$$a \stackrel{\pi}{\sim} b \Leftrightarrow t(a) = t(b)$$

Since the relation π is an equivalent relation, we obtain the quotient sets by

$$A/\pi = \{[a]_\pi : a \in A\} = \oplus_{\mathbf{x} \in V} A_{\mathbf{x}},$$

From this partition of A , we set the orthogonal decomposition of \mathcal{A} into

$$\mathcal{A} = \bigoplus_{\mathbf{x} \in V} \mathcal{A}_{\mathbf{x}}.$$

Here

$$\mathcal{A}_{\mathbf{x}} = \{\psi \in \mathcal{A} \mid a \notin A_{\mathbf{x}} \Rightarrow \psi(a) = 0\},$$

- (2) Time evolution: We assign the local unitary operator on $\mathcal{A}_{\mathbf{x}}$ for each $\mathbf{x} \in V$ which acts alternatively to horizontal and vertical directions so that

$$\begin{aligned} C_{\mathbf{x}} \delta_{(\mathbf{x}; 0)} &= \cos \beta \delta_{(\mathbf{x}; 3)} + \sin \beta \delta_{(\mathbf{x}; 2)}, \\ C_{\mathbf{x}} \delta_{(\mathbf{x}; 1)} &= -\sin \beta \delta_{(\mathbf{x}; 3)} + \cos \beta \delta_{(\mathbf{x}; 2)}, \\ C_{\mathbf{x}} \delta_{(\mathbf{x}; 2)} &= \cos \alpha \delta_{(\mathbf{x}; 1)} + \sin \alpha \delta_{(\mathbf{x}; 0)}, \\ C_{\mathbf{x}} \delta_{(\mathbf{x}; 3)} &= -\sin \alpha \delta_{(\mathbf{x}; 1)} + \cos \alpha \delta_{(\mathbf{x}; 0)}. \end{aligned}$$

The pair of parameters $(\alpha, \beta) \in [0, 2\pi)^2$ which determines this quantum walk will be important to provide the behavior of this walk. The time evolution is denoted by the iteration of the unitary map $U : \mathcal{A} \rightarrow \mathcal{A}$:

$$(U\psi)(a) = \sum_{b:t(b)=o(a)} \langle \delta_{\bar{a}}, C_{o(a)} \delta_b \rangle \psi(b). \quad (2.1)$$

See also figure 1.

- (3) Distribution: Throughout this paper, we fix the initial state $\psi_0 \in \mathcal{A}$ by $\psi_0(a) = \delta_{(\mathbf{0};1)}(a)$ which represents the self loop at the origin. We define the distribution at each time step n , $\rho_n : A \rightarrow [0, 1]$, by

$$\rho_n(a) = |\psi_n(a)|^2.$$

Here $\psi_n = U^{2n}\psi_0$. We observe how this quantum walk recognizes the boundary of the graph through an asymptotic behavior of $\nu_n(j) := \rho_n((0, j); 1)$ for large n .

Remark 1. The unitarity of the time evolution U is immediately shown by the product of the two unitary operators of U ; $U = SC$, where

$$S\psi(a) = \psi(\bar{a}), \quad C = \bigoplus_{\mathbf{x} \in V} C_{\mathbf{x}}. \quad (2.2)$$

The unitary operators S and C are called shift and coin operators, respectively.

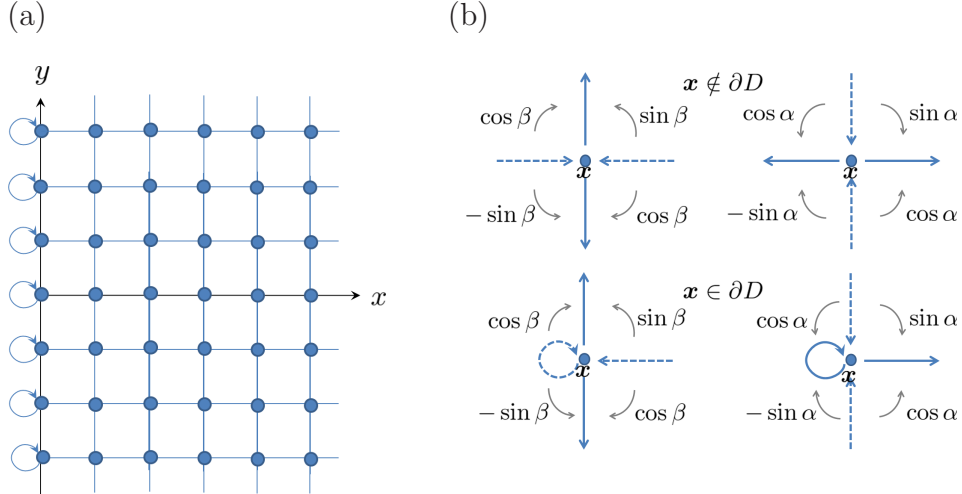


Figure 1: (a) The graph treated in the present work. (b) The one-step time evolution U at a vertex $\mathbf{x} \notin \partial D$ and $\mathbf{x} \in \partial D$. The dotted and solid arcs represent the input and output arcs, respectively.

2.3 An alternative quantum walk

The horizontal arcs and the vertical arcs are denoted by

$$A^{(\leftrightarrow)} = \{(\mathbf{x}; d) \in A \mid d \in \{0, 1\}\}, \quad A^{(\updownarrow)} = \{(\mathbf{x}; d) \in A \mid d \in \{2, 3\}\},$$

respectively. We set the associated subspaces

$$\mathcal{A}^{(\leftrightarrow)} = \{\psi \in \mathcal{A} \mid a \notin A^{(\leftrightarrow)} \Rightarrow \psi(a) = 0\}, \quad \mathcal{A}^{(\updownarrow)} = \{\psi \in \mathcal{A} \mid a \notin A^{(\updownarrow)} \Rightarrow \psi(a) = 0\}.$$

We define a unitary map \mathcal{U} which converts the Hilbert space in the arc set representation to one in the vertex set with four internal states representation $\mathcal{U} : \mathcal{A} \rightarrow \ell^2(V; \mathbb{C}^4)$ and $\mathcal{U}_e : \mathcal{A}^{(\leftrightarrow)} \rightarrow \ell^2(V; \mathbb{C}^2)$, where

$$\ell^2(V; \mathbb{C}^n) = \{f : V \rightarrow \mathbb{C}^n \mid \sum_{\mathbf{x} \in V} \|f(\mathbf{x})\|_{\mathbb{C}^n}^2 < \infty\} \quad (n \in \{1, 2, \dots\}).$$

Definition 1.

We define $\mathcal{U} : \mathcal{A} \rightarrow \ell^2(V; \mathbb{C}^4)$ such that

$$(\mathcal{U}\psi)(\mathbf{x}) = {}^T[\psi(\mathbf{x}; 0) \ \psi(\mathbf{x}; 1) \ \psi(\mathbf{x}; 2) \ \psi(\mathbf{x}; 3)].$$

We also define $\mathcal{U}_e : \mathcal{A}^{(\leftrightarrow)} \rightarrow \ell^2(V; \mathbb{C}^2)$ such that

$$(\mathcal{U}_e\psi)(\mathbf{x}) = {}^T[\psi(\mathbf{x}; 0) \ \psi(\mathbf{x}; 1)].$$

We can see that these inverse maps $\mathcal{U}^{-1} : \ell^2(V; \mathbb{C}^4) \rightarrow \mathcal{A}$ and $\mathcal{U}_e^{-1} : \ell^2(V; \mathbb{C}^2) \rightarrow \mathcal{A}^{(\leftrightarrow)}$ are expressed by

$$\begin{aligned} (\mathcal{U}^{-1}f)(\mathbf{x}; j) &= f_j(\mathbf{x}) \quad (j \in \{0, 1, 2, 3\}), \\ (\mathcal{U}_e^{-1}g)(\mathbf{x}; j) &= g_j(\mathbf{x}) \quad (j \in \{0, 1\}) \end{aligned}$$

for $f \in \ell^2(V; \mathbb{C}^4)$ with $f(\mathbf{y}) = {}^T[f_0(\mathbf{y}) \ f_1(\mathbf{y}) \ f_2(\mathbf{y}) \ f_3(\mathbf{y})] \in \mathbb{C}^4$ and $g \in \ell^2(V; \mathbb{C}^2)$ with $g(\mathbf{y}) = {}^T[g_0(\mathbf{y}) \ g_1(\mathbf{y})] \in \mathbb{C}^2$. We put $|0\rangle = {}^T[1, 0]$ and $|1\rangle = {}^T[0, 1]$ as the standard basis of \mathbb{C}^2 . Set the two-dimensional γ -rotation matrix by

$$H_\gamma = \begin{bmatrix} \cos \gamma & -\sin \gamma \\ \sin \gamma & \cos \gamma \end{bmatrix}. \quad (\gamma \in [0, 2\pi))$$

We define

$$P_\gamma = |0\rangle\langle 0|H_\gamma, \quad Q_\gamma = |1\rangle\langle 1|H_\gamma, \quad S_\gamma = |1\rangle\langle 0|H_\gamma.$$

For $\psi \in \ell^2(V; \mathbb{C}^4)$ with $\psi(\mathbf{x}) = {}^T[\psi_0(\mathbf{x}) \ \psi_1(\mathbf{x}) \ \psi_2(\mathbf{x}) \ \psi_3(\mathbf{x})] \in \mathbb{C}^4$, we denote $\psi^{(\leftrightarrow)}(\mathbf{x}) = {}^T[\psi_0(\mathbf{x}) \ \psi_1(\mathbf{x}) \ 0 \ 0]$ and $\psi^{(\updownarrow)}(\mathbf{x}) = {}^T[0 \ 0 \ \psi_2(\mathbf{x}) \ \psi_3(\mathbf{x})]$.

Lemma 1. Denote $U' = \mathcal{U}\mathcal{U}\mathcal{U}^{-1}$. Then we have

$$(U'\psi^{(\leftrightarrow)})(x, y) = \tilde{Q}_\beta\psi^{(\leftrightarrow)}(x, y-1) + \tilde{P}_\beta\psi^{(\leftrightarrow)}(x, y+1) \quad (2.3)$$

$$(U'\psi^{(\updownarrow)})(x, y) = \begin{cases} \tilde{Q}_\alpha\psi^{(\updownarrow)}(x-1, y) + \tilde{P}_\alpha\psi^{(\updownarrow)}(x+1, y) & : (x, y) \notin \partial D, \\ \tilde{S}_\alpha\psi^{(\updownarrow)}(x, y) + \tilde{P}_\alpha\psi^{(\updownarrow)}(x+1, y) & : (x, y) \in \partial D. \end{cases} \quad (2.4)$$

Here

$$\tilde{P}_\alpha := |0\rangle\langle 1| \otimes P_\alpha, \quad \tilde{Q}_\alpha := |0\rangle\langle 1| \otimes Q_\alpha, \quad \tilde{P}_\beta := |1\rangle\langle 0| \otimes P_\beta, \quad \tilde{Q}_\beta := |1\rangle\langle 0| \otimes Q_\beta, \quad \tilde{S}_\alpha := |0\rangle\langle 1| \otimes S_\alpha.$$

Proof. We put $C' = \mathcal{U}C\mathcal{U}^{-1}$ and $S' = \mathcal{U}S\mathcal{U}^{-1}$. By the bipartiteness of the coin operator C with respect to “ $\{0, 1\}$ ” and “ $\{2, 3\}$ ” directions, it holds that for every $\phi \in \mathcal{A}$,

$$\begin{bmatrix} (C\phi)(\mathbf{x}; 0) \\ (C\phi)(\mathbf{x}; 1) \end{bmatrix} = \sigma_1 H_\alpha \begin{bmatrix} \phi(\mathbf{x}; 2) \\ \phi(\mathbf{x}; 3) \end{bmatrix}, \quad \begin{bmatrix} (C\phi)(\mathbf{x}; 2) \\ (C\phi)(\mathbf{x}; 3) \end{bmatrix} = \sigma_1 H_\beta \begin{bmatrix} \phi(\mathbf{x}; 0) \\ \phi(\mathbf{x}; 1) \end{bmatrix}. \quad (2.5)$$

Here $\sigma_1 = |0\rangle\langle 1| + |1\rangle\langle 0|$. Using this, we have for every $\psi \in \ell^2(V; \mathbb{C}^4)$ with $\psi(\mathbf{x}) = {}^T[\psi_0(\mathbf{x}), \dots, \psi_3(\mathbf{x})]$,

$$(C'\psi)(\mathbf{x}) = |0\rangle \otimes \sigma_1 H_\alpha \begin{bmatrix} \psi_2(\mathbf{x}) \\ \psi_3(\mathbf{x}) \end{bmatrix} + |1\rangle \otimes \sigma_1 H_\beta \begin{bmatrix} \psi_0(\mathbf{x}) \\ \psi_1(\mathbf{x}) \end{bmatrix}. \quad (2.6)$$

Concerning the shift operator S flipping the arc direction; $(S\phi)(a) = \phi(\bar{a})$, we have

$$(S'\psi)(x, y) = \begin{cases} {}^T[\psi_1(x+1, y) & \psi_0(x-1, y) & \psi_3(x, y+1) & \psi_2(x, y-1)] & : (x, y) \notin \partial D, \\ {}^T[\psi_1(x+1, y) & \psi_1(x, y) & \psi_3(x, y+1) & \psi_2(x, y-1)] & : (x, y) \in \partial D. \end{cases} \quad (2.7)$$

By (2.6) and (2.7), we have

$$\begin{aligned} (U'\psi)(x, y) &= \tilde{P}_\alpha \psi^{(\uparrow)}(x+1, y) + \tilde{Q}_\alpha \psi^{(\uparrow)}(x-1, y) \\ &\quad + \tilde{P}_\beta \psi^{(\leftrightarrow)}(x, y+1) + \tilde{Q}_\beta \psi^{(\leftrightarrow)}(x, y-1), \quad ((x, y) \notin \partial D), \end{aligned} \quad (2.8)$$

and

$$\begin{aligned} (U'\psi)(x, y) &= \tilde{P}_\alpha \psi^{(\uparrow)}(x+1, y) + \tilde{S}_\alpha \psi^{(\uparrow)}(x, y) \\ &\quad + \tilde{P}_\beta \psi^{(\leftrightarrow)}(x, y+1) + \tilde{Q}_\beta \psi^{(\leftrightarrow)}(x, y-1), \quad ((x, y) \in \partial D). \end{aligned} \quad (2.9)$$

Then we have the desired conclusion. \square

For clarity, we mention the connection between the above description of the coin and the shift operators and the commonly used description of the coin and the shift operators, C'' and S'' , respectively, such as in Ref. [4]. We regard four internal states in the vertex representation as the left, right, down, and up mover components,

$$|L\rangle = {}^T[1, 0, 0, 0], \quad |R\rangle = {}^T[0, 1, 0, 0], \quad |D\rangle = {}^T[0, 0, 1, 0], \quad |U\rangle = {}^T[0, 0, 0, 1],$$

respectively, and the position (x, y) is described by

$$|x, y\rangle.$$

On this basis, the coin operator C' is described by

$$C' = \sum_{x, y} |x, y\rangle\langle x, y| \otimes \begin{bmatrix} 0 & \sigma_1 H_\alpha \\ \sigma_1 H_\beta & 0 \end{bmatrix} : (x, y) \in V.$$

while the common descriptions of C'' and S'' are

$$C'' = \sum_{x, y} |x, y\rangle\langle x, y| \otimes \begin{bmatrix} 0 & H_\alpha \\ H_\beta & 0 \end{bmatrix} : (x, y) \in V.$$

and

$$\begin{aligned}
S''|x, y\rangle|R\rangle &= |x+1, y\rangle|R\rangle, \\
S''|x, y\rangle|D\rangle &= |x, y-1\rangle|D\rangle, \\
S''|x, y\rangle|U\rangle &= |x, y+1\rangle|U\rangle, \\
S''|x, y\rangle|L\rangle &= \begin{cases} |x-1, y\rangle|L\rangle & : (x, y) \notin \partial D, \\ |x, y\rangle|R\rangle & : (x, y) \in \partial D, \end{cases}
\end{aligned} \tag{2.10}$$

respectively. Rewriting the time-evolution operator U' , we have

$$U' = S'C' = S''(S''^{-1}S'C'). \tag{2.11}$$

Taking into account the different order of internal states in the basis, $S''^{-1}S'$ is expressed by

$$S''^{-1}S' = \sum_{x,y} |x, y\rangle\langle x, y| \otimes \begin{bmatrix} \sigma_1 & 0 \\ 0 & \sigma_1 \end{bmatrix},$$

and we confirm the relation

$$C'' = S''^{-1}S'C'. \tag{2.12}$$

From (2.11) and (2.12), without loss of generality, we can alternatively describe the model as $U' = S''C''$ instead of $U' = S'C'$ in the vertex representation.

The property that if $\gamma = \gamma'$, then $\tilde{X}_\gamma \tilde{X}'_{\gamma'} = 0$ ($X, X' \in \{P, Q\}$) reflects that the quantum walker moves to vertical and horizontal directions, alternatively. Therefore we can easily observe that

$$U^2(\mathcal{A}^{(\leftrightarrow)}) \subset \mathcal{A}^{(\leftrightarrow)}, \quad U^2(\mathcal{A}^{(\dagger)}) \subset \mathcal{A}^{(\dagger)}.$$

Since our initial condition is $\psi_0 = \delta_{(0;1)} \in \mathcal{A}^{(\leftrightarrow)}$ which is the self loop at the origin, we concentrate on $\mathcal{A}^{(\leftrightarrow)}$. By using Lemma 1, we obtain Lemma 2.

Lemma 2. *Let $\Gamma : \ell^2(V; \mathbb{C}^2) \rightarrow \ell^2(V; \mathbb{C}^2)$ be a map defined by for $\varphi \in \ell^2(V; \mathbb{C}^2)$,*

$$\begin{aligned}
(\Gamma\varphi)(x, y) &= Q_\alpha Q_\beta \varphi(x-1, y-1) + Q_\alpha P_\beta \varphi(x-1, y+1) \\
&\quad + P_\alpha Q_\beta \varphi(x+1, y-1) + P_\alpha P_\beta \varphi(x+1, y+1), \quad ((x, y) \notin \partial D),
\end{aligned} \tag{2.13}$$

and

$$\begin{aligned}
(\Gamma\varphi)(x, y) &= S_\alpha Q_\beta \varphi(x, y-1) + S_\alpha P_\beta \varphi(x, y+1) \\
&\quad + P_\alpha Q_\beta \varphi(x+1, y-1) + P_\alpha P_\beta \varphi(x+1, y+1), \quad ((x, y) \in \partial D).
\end{aligned} \tag{2.14}$$

Then we have

$$U^2|_{\mathcal{A}^{(\leftrightarrow)}} = \mathcal{U}_e^{-1} \Gamma \mathcal{U}_e.$$

Proof. For $\psi = \psi^{(\leftrightarrow)} \in \ell^2(V; \mathbb{C}^4)$, first we examine $(U'^2\psi)(x, y)$. We should remark that

$$(U'\psi^{(\leftrightarrow)})(x, y) = (U'\psi)^{(\dagger)}(x, y), \quad (2.15)$$

because of \tilde{Q}_β and \tilde{P}_β . Thus by (2.4), for $(x, y) \notin \partial D$, we have

$$(U'^2\psi)(x, y) = \tilde{P}_\alpha(U'\psi)^{(\dagger)}(x+1, y) + \tilde{Q}_\alpha(U'\psi)^{(\dagger)}(x-1, y). \quad (2.16)$$

Moreover by (2.3) and (2.15), we have

$$\begin{aligned} (U'^2\psi)(x, y) &= \tilde{P}_\alpha(\tilde{Q}_\beta\psi^{(\leftrightarrow)}(x+1, y-1) + \tilde{P}_\beta\psi^{(\leftrightarrow)}(x+1, y+1)) \\ &\quad + \tilde{Q}_\alpha(\tilde{Q}_\beta\psi^{(\leftrightarrow)}(x-1, y-1) + \tilde{P}_\beta\psi^{(\leftrightarrow)}(x-1, y+1)). \end{aligned} \quad (2.17)$$

Since ψ is expressed by some $\varphi \in \mathcal{U}_e(\mathcal{A}^{(\leftrightarrow)})$ so that $\psi(\mathbf{x}) = |0\rangle \otimes \varphi(\mathbf{x})$ and it holds $\tilde{X}_\alpha\tilde{Y}_\beta = |0\rangle\langle 0| \otimes X_\alpha Y_\beta$ ($X, Y \in \{P, Q\}$), we have

$$\begin{aligned} (U'^2\psi)(x, y) &= |0\rangle \otimes \{P_\alpha Q_\beta \varphi(x+1, y-1) + P_\alpha P_\beta \varphi(x+1, y+1) \\ &\quad + Q_\alpha Q_\beta \varphi(x-1, y-1) + Q_\alpha P_\beta \varphi(x-1, y+1)\}. \end{aligned} \quad (2.18)$$

In the same way for $(x, y) \in \partial D$ case,

$$\begin{aligned} (U'^2\psi)(x, y) &= |0\rangle \otimes \{P_\alpha Q_\beta \varphi(x+1, y-1) + P_\alpha P_\beta \varphi(x+1, y-1) \\ &\quad + S_\alpha Q_\beta \varphi(x, y-1) + S_\alpha P_\beta \varphi(x, y+1)\}, \end{aligned} \quad (2.19)$$

which implies

$$(U'^2\psi)(\mathbf{x}) = |0\rangle \otimes (\Gamma\varphi)(\mathbf{x}), \quad (\forall \mathbf{x} \in V). \quad (2.20)$$

By the way, for any $\phi \in \mathcal{A}^{(\leftrightarrow)}$, we have

$$(U^2|_{\mathcal{A}^{(\leftrightarrow)}}\phi)(\mathbf{x}; j) = (\mathcal{U}^{-1}U'^2\mathcal{U}\phi)(\mathbf{x}, j) = \begin{cases} (U'^2\psi)_j(\mathbf{x}) = (\Gamma\varphi)_j(\mathbf{x}) & : j \in \{0, 1\} \\ 0 & : j \in \{2, 3\}. \end{cases}$$

where $\psi(\mathbf{x}) = (\mathcal{U}\phi)(\mathbf{x}) = |0\rangle \otimes \varphi(\mathbf{x})$. Here in the last equality, we used (2.20). Remarking $\mathcal{U}\mathcal{U}_e^{-1}\varphi = \varphi$, we have

$$(\mathcal{U}_e U^2|_{\mathcal{A}^{(\leftrightarrow)}}\mathcal{U}_e^{-1}\varphi)(\mathbf{x}) = \begin{bmatrix} (U^2|_{\mathcal{A}^{(\leftrightarrow)}}\mathcal{U}_e^{-1}\varphi)(\mathbf{x}; 0) \\ (U^2|_{\mathcal{A}^{(\leftrightarrow)}}\mathcal{U}_e^{-1}\varphi)(\mathbf{x}; 1) \end{bmatrix} = \begin{bmatrix} (\Gamma\varphi)_0(\mathbf{x}) \\ (\Gamma\varphi)_1(\mathbf{x}) \end{bmatrix} = (\Gamma\varphi)(\mathbf{x}),$$

which completes the proof. \square

The notion of the weights of matrices P , Q and S associated with the one-step moving to the neighbor vertex, comes from a quantum analogue of a discrete-time random walk [14] and becomes useful to take the Fourier analysis in the next section. From now on, by Lemma 1, we will focus on the unitary operator Γ on $\ell^2(V; \mathbb{C}^2)$ instead of the unitary operator U on \mathcal{A} .

3 Connecting the CMV matrix

By the previous section, the model is reduced to the quantum walk on $\ell^2(V; \mathbb{C}^2)$ that the walker moves to the neighbor with the two-dimensional matrix weight following the unitary time evolution Γ . One of the keys in this paper is a connection between AE model and the CMV matrix [7]. To show the connection, we prepare the following two maps. Set $L^2(\mathbb{Z}_+ \times [0, 2\pi); \mathbb{C}^2)$ by $\{\hat{\varphi} : \mathbb{Z}_+ \times [0, 2\pi) \rightarrow \mathbb{C}^2 \mid \sum_{j \in \mathbb{Z}_+} \int_0^{2\pi} \|\hat{\varphi}(j; k)\|_{\mathbb{C}^2}^2 dk < \infty\}$.

Definition 2. Let $\mathcal{F} : \ell^2(V; \mathbb{C}^2) \rightarrow L^2(\mathbb{Z}_+ \times [0, 2\pi); \mathbb{C}^2)$ be the Fourier transform defined by

$$\hat{\varphi}(j; k) := (\mathcal{F}\varphi)(j; k) = \sum_{m \in \mathbb{Z}} \varphi(j, m) e^{ikm} \quad (j \in \mathbb{Z}, k \in [0, 2\pi)),$$

and for fixed $k \in [0, 2\pi)$ it can be written that $\varphi'(\cdot) = \hat{\varphi}(\cdot; k)$.

Definition 3. For fixed $k \in [0, 2\pi)$, let $\Lambda_k : \ell^2(\mathbb{Z}_+; \mathbb{C}^2) \rightarrow \ell^2(\mathbb{Z}_+)$ be defined by

$$(\Lambda_k \varphi')(j) = e^{i\omega(j)} \times \begin{cases} \langle 1 | \varphi'([j/2]) \rangle & : j \text{ is even,} \\ \langle 0 | \varphi'([j/2]) \rangle & : j \text{ is odd.} \end{cases}$$

Here $[a]$ is the minimum integer so that $[a] \leq a$ for $a \in \mathbb{R}$ and

$$\omega(2j) = -j \arg(\langle 0 | \hat{H}_k | 0 \rangle), \quad \omega(2j+1) = (j+1) \arg(\langle 1 | \hat{H}_k | 1 \rangle),$$

where $\hat{H}_k \in \text{SU}(2)$ is defined in (3.3).

Remark 2. The inverse maps of $\mathcal{F}^{-1} : L^2(\mathbb{Z}_+ \times [0, 2\pi); \mathbb{C}^2) \rightarrow \ell^2(V; \mathbb{C}^2)$ and $\Lambda_k^{-1} : \ell^2(\mathbb{Z}_+) \rightarrow \ell^2(\mathbb{Z}_+; \mathbb{C}^2)$ are

$$\begin{aligned} (\mathcal{F}^{-1}\hat{\varphi})(x, y) &= \int_0^{2\pi} \hat{\varphi}(x; k) e^{-iky} \frac{dk}{2\pi}, \\ (\Lambda_k^{-1}f)(j) &= \begin{bmatrix} e^{-i\omega(2j+1)} f(2j+1) \\ e^{-i\omega(2j)} f(2j) \end{bmatrix}. \end{aligned}$$

Remark 3. For every $\hat{\varphi} \in L^2(\mathbb{Z}_+ \times [0, 2\pi); \mathbb{C}^2)$, by the Fubini's theorem,

- (1) $\Lambda_k \hat{\varphi}$ is well-defined, because $\hat{\varphi}(\cdot; k) = \varphi'(\cdot)$ belongs to $\ell^2(\mathbb{Z}_+; \mathbb{C}^2)$ for fixed $k \in [0, 2\pi)$;
- (2) for every unitary operator E on $\ell^2(\mathbb{Z}_+)$, we have $\Lambda_k^{-1} E \Lambda_k \hat{\varphi}(\cdot; k) \in \ell^2(V; \mathbb{C}^2)$ for fixed k , and $\Lambda_k^{-1} E \Lambda_k \hat{\varphi} \in L^2(\mathbb{Z}_+ \times [0, 2\pi); \mathbb{C}^2)$.

Now we can state the following theorem. Recall that $\Gamma = \mathcal{U}_e U^2|_{\mathcal{A}(\leftrightarrow)} \mathcal{U}_e^{-1}$.

Theorem 1. Denote \mathcal{C}_k be the CMV matrix whose Verblunsky parameter is $(\eta(k), 0, \eta(k), 0, \dots)$, where $\eta(k) = \sin(\alpha - \beta) \cos k + i \sin(\alpha + \beta) \sin k$. Then we have

$$(\Gamma^n \varphi)(x, y) = \int_0^{2\pi} (\Lambda_k^{-1T} \mathcal{C}_k^n \Lambda_k \hat{\varphi})(x) e^{-iky} \frac{dk}{2\pi}, \quad ((x, y) \in V). \quad (3.1)$$

Before giving the proof of this theorem, we take a short review on the CMV matrix which is a unitary operator on $\ell^2(\mathbb{Z}_+)$ as follows.

3.1 The CMV matrix

Denote \mathbb{T} as the unit circle on the complex plane, that is, $\mathbb{T} = \{z \in \mathbb{C} \mid |z| = 1\}$. For given a spectral measure on \mathbb{T} , we set the Hilbert space $L^2_\mu(\mathbb{T})$ whose inner product is defined by

$$\langle f, g \rangle_\mu = \int_{z \in \mathbb{T}} \overline{f(z)} g(z) d\mu(z).$$

Let $\{\chi_j(z)\}_{j=0}^\infty \subset L^2_\mu(\mathbb{T})$ be the orthogonal Laurent polynomials associated with the spectral measure $d\mu(z)$ on the unit circle in the complex plane obtained by the orthogonalization of $\{1, z, z^{-1}, z^2, \dots\}$. The CMV matrix \mathcal{C} is expressed by

$$(\mathcal{C})_{i,j} = \langle \chi_i, z \chi_j \rangle_\mu$$

which represents an canonical representation of multiplication operation on $L^2_\mu(\mathbb{T})$; $f(z) \mapsto zf(z)$. The CMV matrix has a one-to-one correspondence between called the Verblunsky parameters $(\eta_0, \eta_1, \eta_2, \dots)$. The simplest matrix representation (η_0, η_1, \dots) is given by the following form [5, 6]:

$$\mathcal{C} = \begin{bmatrix} \overline{\eta}_0 & \rho_0 \overline{\eta}_1 & \rho_0 \rho_1 & 0 & 0 & 0 & 0 & 0 & \dots \\ \rho_0 & -\eta_0 \overline{\eta}_1 & -\eta_0 \rho_1 & 0 & 0 & 0 & 0 & 0 & \dots \\ 0 & \rho_1 \overline{\eta}_2 & -\eta_1 \overline{\eta}_2 & \rho_2 \overline{\eta}_3 & \rho_2 \rho_3 & 0 & 0 & 0 & \dots \\ 0 & \rho_1 \rho_2 & -\eta_1 \rho_2 & -\eta_2 \overline{\eta}_3 & -\eta_2 \rho_3 & 0 & 0 & 0 & \dots \\ 0 & 0 & 0 & \rho_3 \overline{\eta}_4 & -\eta_3 \overline{\eta}_4 & \rho_4 \overline{\eta}_5 & \rho_4 \rho_5 & 0 & \dots \\ 0 & 0 & 0 & \rho_3 \rho_4 & -\eta_3 \rho_4 & -\eta_4 \overline{\eta}_5 & -\eta_4 \rho_5 & 0 & \dots \\ & \vdots & \vdots & \vdots & \vdots & \vdots & \ddots & & \end{bmatrix},$$

where $\eta_j \in \mathbb{C}$ satisfies $|\alpha_j| < 1$ and $\rho_j = \sqrt{1 - |\alpha_j|^2}$.

3.2 Reduction to a quantum walk on the half line: Type I quantum walk

For fixed $k \in [0, 2\pi)$, we define $\hat{\Gamma}_k : \ell^2(\mathbb{Z}; \mathbb{C}^2) \rightarrow \ell^2(\mathbb{Z}; \mathbb{C}^2)$ by

$$(\hat{\Gamma}_k \varphi')(x) = \begin{cases} \hat{P}_k \varphi'(x+1) + \hat{Q}_k \varphi'(x-1) & : x \geq 1, \\ \hat{P}_k \varphi'(x+1) + \hat{S}_k \varphi'(x) & : x = 0, \end{cases} \quad (3.2)$$

where $\hat{P}_k = |0\rangle\langle 0| \hat{H}_k$, $\hat{Q}_k = |1\rangle\langle 1| \hat{H}_k$ and $\hat{S}_k = |1\rangle\langle 0| \hat{H}_k$. Here \hat{H}_k is defined by $H_\alpha \hat{D}(k) H_\beta$, where

$$\hat{D}_k = \begin{bmatrix} e^{-ik} & 0 \\ 0 & e^{ik} \end{bmatrix}.$$

More precisely,

$$\hat{H}_k = \begin{bmatrix} e^{-ik} \cos \alpha \cos \beta - e^{ik} \sin \alpha \sin \beta & -e^{-ik} \cos \alpha \sin \beta - e^{ik} \sin \alpha \cos \beta \\ e^{-ik} \sin \alpha \cos \beta + e^{ik} \cos \alpha \sin \beta & -e^{-ik} \sin \alpha \sin \beta + e^{ik} \cos \alpha \cos \beta \end{bmatrix}. \quad (3.3)$$

Lemma 3. Let $\varphi_n \in \ell^2(V; \mathbb{C}^2)$ be the n -th iteration of Γ with the initial state $\varphi_0(\mathbf{x}) = \delta(\mathbf{x})^T[0, 1]$, that is, $\varphi_n = \Gamma^n \varphi_0$. The Fourier transform of φ_n described by $\mathcal{F}(\varphi_n) = \hat{\varphi}_n \in L^2(\mathbb{Z} \times [0, 2\pi); \mathbb{C}^2)$ is expressed by

$$\hat{\varphi}_n = \hat{\Gamma}_k^n \hat{\varphi}_0, \quad \hat{\varphi}_0 = \delta(x)^T[0, 1]. \quad (3.4)$$

Proof. Due to the shift invariance with respect to the vertical direction and Lemma 2, we immediately obtain the conclusion. \square

We introduce the type I quantum walk deriving from the CMV matrix in the following. Let A' be the arc set of \mathbb{Z}_+ with the self loop at the origin, that is,

$$A' = \{(j; 0), (j; 1) \mid j \in \mathbb{Z}_+\}.$$

Here $(j; 0)$ indicates the arc from $j + 1$ to x , and $(j; 1)$ indicates the arc from $j - 1$ to j for $j \geq 1$, and the self loop for $j = 0$. We define the subsets of A' by

$$A'_j = \{(j; 0), (j; 1)\}.$$

Definition 4. The Type I quantum walk [7, 19] is defined as follows:

- (1) Total state space: $\mathcal{A}' = \ell^2(A')$
- (2) Time evolution: We set $\mathcal{A}'_j = \{\varphi' \in \mathcal{A}' \mid a \notin A_j \Rightarrow \varphi'(a) = 0\}$. The local unitary operator on \mathcal{A}'_j is defined by

$$C'_j \cong \begin{bmatrix} c & d \\ a & b \end{bmatrix} \quad (3.5)$$

$$(3.6)$$

setting the canonical basis of \mathcal{A}'_j by $\{\delta_{(j;0)}, \delta_{(j;1)}\}$ in this order. The time evolution $W : \mathcal{A}' \rightarrow \mathcal{A}'$ is described by

$$(W\psi)(a) = \sum_{b: t(a)=o(b)} \langle \delta_a, C'_j \delta_b \rangle \psi(b). \quad (3.7)$$

As is the previous section, we also define $\mathcal{U}' : \ell^2(A') \rightarrow \ell^2(\mathbb{Z}_+; \mathbb{C}^2)$ as follows:

$$(\mathcal{U}'\psi)(x) = {}^T[\psi(x; 0), \psi(x; 1)] \quad (x \in \mathbb{Z}, j \in \{0, 1\}).$$

The inverse map is $(\mathcal{U}'^{-1}\varphi)(x; j) = \varphi_j(x)$. Putting $\Gamma' = \mathcal{U}'W\mathcal{U}'^{-1}$, we take the n -th iteration of Γ' as φ'_n with the initial state φ'_0 , that is, $\varphi'_n = \Gamma'^n \varphi'_0$. From a simple observation, we have

$$\varphi'_{n+1}(j) = \begin{cases} Q\varphi'_n(j-1) + P\varphi'_n(j+1) & : j \geq 1, \\ S\varphi'_n(j) + P\varphi'_n(j+1) & : j = 0. \end{cases} \quad (3.8)$$

Here $P = |0\rangle\langle 0|H$, $Q = |1\rangle\langle 1|H$ and $S = |0\rangle\langle 1|H$ with

$$H = \begin{bmatrix} a & b \\ c & d \end{bmatrix} \in \text{U}(2).$$

Therefore $\mathcal{U}'\hat{\Gamma}_k\mathcal{U}'^{-1}$ is identical with the time evolution of the Type I quantum walk in the case of $H = \hat{H}_k$ for fixed k . Mapping the time iteration of $\hat{\Gamma}_k$ to the Type I quantum walk's one has the following benefit.

Lemma 4. [7, 19] For given type I quantum walk with the local unitary coin C'_j (3.5), let $\mathcal{D} : \mathcal{A}' \rightarrow \ell^2(\mathbb{Z}_+)$ be*

$$(\mathcal{D}\psi)(m) = \begin{cases} \psi((m+1)/2; 0)e^{i\arg(a)(m+1)/2} & : m \text{ is odd,} \\ \psi(m/2; 1)e^{-i\arg(d)m/2} & : m \text{ is even.} \end{cases}$$

The time evolution of Type I quantum walk, W , is unitary equivalent to the CMV matrix with null odd Verblunsky parameter $(\eta_0, 0, \eta_2, 0, \eta_4, 0, \dots)$, that is,

$$W = \mathcal{D}^T \mathcal{C} \mathcal{D}^{-1},$$

where

$$\eta_j = \begin{cases} \eta \Delta^{-(j+1)/2} & : j \text{ is even,} \\ 0 & : \text{otherwise,} \end{cases} \quad (3.9)$$

with $\eta = \Delta^{1/2}\bar{b}$, $\Delta = ad - bc$.

Now we are in the place of the proof of Theorem 1.

Proof of Theorem 1

Since $\det(H_\alpha) = \det(H_\beta) = \det(\hat{D}_k) = 1$, we have $\Delta = \det(\hat{H}_k) = 1$. Thus concerning our local quantum coin (3.3), the corresponding Verblunsky parameter is $\eta_j = \eta(k)$ (j is even), where

$$\eta(k) = \overline{\langle 0 | \hat{H}_k | 1 \rangle} = -\cos k \sin(\alpha + \beta) + i \sin k \sin(\alpha - \beta). \quad (3.10)$$

By Lemma 4,

$$\mathcal{U}' \hat{\Gamma}_k \mathcal{U}'^{-1} = \mathcal{D}^{-1T} \mathcal{C}_k \mathcal{D}. \quad (3.11)$$

Remarking that $\Lambda_k = \mathcal{D} \mathcal{U}'$, we have

$$\Lambda_k^{-1T} \mathcal{C}_k^n \Lambda_k \hat{\varphi}_0 = \hat{\varphi}_n. \quad (3.12)$$

Taking the Fourier inverse to the above, that is,

$$\varphi(x, y) = \int_0^{2\pi} \hat{\varphi}_n(x; k) e^{-iky},$$

we obtain the desired conclusion. \square

*The inverse map $\mathcal{D}^{-1} : \ell^2(\mathbb{Z}_+) \rightarrow \mathcal{A}'$ is

$$(\mathcal{D}f)(m; j) = \begin{cases} f(2m+1)e^{-i(2m+1)\arg(a)} & : j = 0, \\ f(2m)e^{i2m\arg(d)} & : j = 1. \end{cases}$$

4 Dispersion Relations and Topological Phases

4.1 Dispersion relations

First, we set important values for our model in advance:

$$\rho(k) := \sqrt{1 - |\eta(k)|^2} = \sqrt{\cos^2(\alpha - \beta) - \sin 2\alpha \sin 2\beta \cos^2 k}, \quad (4.1)$$

$$m_0(k) := m_0 = \begin{cases} \frac{|\cos k \sin(\alpha + \beta)|}{\sqrt{1 - \sin^2(\alpha - \beta) \sin^2 k}} & : \rho(k) \neq 0, \\ 1 & : \rho(k) = 0, \end{cases} \quad (4.2)$$

$$\theta_0(k) := \begin{cases} \arcsin(-\sin k \sin(\alpha - \beta)) & : \cos k \sin(\alpha + \beta) \leq 0, \\ \pi - \arcsin(-\sin k \sin(\alpha - \beta)) & : \cos k \sin(\alpha + \beta) > 0. \end{cases} \quad (4.3)$$

Let us define $Bu, Ed \in [0, 2\pi)^2$ as follows. We call Bu and Ed “bulk” and “edge”, respectively. We call the parameter $k \in [0, 2\pi)$ in (4.15) (4.16) wave number. The dispersion relation of this quantum walk is described by $Bu \cup Ed$.

Definition 5. Let $\sigma_c^{(k)}$ and $\sigma_p^{(k)}$ be the continuous and point spectrum's of $\hat{\Gamma}_k$ for fixed k . Then we set

$$Bu = \bigcup_{k \in [0, 2\pi)} \{(k, \theta) \mid \theta \in \sigma_c^{(k)}\}, \quad (4.4)$$

$$Ed = \bigcup_{k \in [0, 2\pi)} \{(k, \theta) \mid \theta \in \sigma_p^{(k)}\}. \quad (4.5)$$

We have detailed expression of the spectrum of $\hat{\Gamma}_k$ as follows.

Lemma 5. For fixed $k \in [0, 2\pi)$, the spectrum of $\hat{\Gamma}_k$ is decomposed into continuous spectrum $\sigma_c^{(k)}$ and point spectrum $\sigma_p^{(k)}$, that is, $\sigma(\hat{\Gamma}_k) = \sigma_c^{(k)} \oplus \sigma_p^{(k)}$, where

$$\sigma_c^{(k)} = \{\theta \in [0, 2\pi) \mid |\cos \theta| \leq \rho(k)\} \quad (4.6)$$

$$\sigma_p^{(k)} = \begin{cases} \{\theta_0(k)\} & : \sin(\alpha - \beta) \neq 0, k \notin \{\pi/2, 3\pi/2\}, \\ \emptyset & : \text{otherwise.} \end{cases} \quad (4.7)$$

Moreover we have

$$\sigma(U^2|_{\mathcal{A}^{(\leftrightarrow)}}) = \bigcup_{k \in [0, 2\pi)} (\sigma_c^{(k)} \cup \sigma_p^{(k)}). \quad (4.8)$$

Proof. The detailed spectrum of this CMV matrix has been already obtained by [7, 19]. We provide partially the results as follows.

Lemma 6. [7, 19] The spectral measure of the CMV matrix with the Verblunsky parameter $(\eta, 0, \eta, 0, \dots)$ is described as follows.

(1) For $|\eta| = 1$ case.

$$d\mu(\theta) = \delta(\theta + \arccos(\eta)). \quad (4.9)$$

(2) For $|\eta| < 1$ case.

$$d\mu(\theta) = w(\theta) \frac{d\theta}{2\pi} + m_0 \delta(\theta - \theta_0). \quad (4.10)$$

Here $w(\theta)$ is an absolutely continuous part

$$w(\theta) = \frac{\sqrt{\rho^2 - \cos^2 \theta}}{|\sin \theta + \operatorname{Im}(\eta)|} \mathbf{1}_{\{|\cos \theta| < \rho\}}(\theta), \quad (\rho = \sqrt{1 - |\eta|^2}) \quad (4.11)$$

and $m_0 \in [0, 1]$ is the mass at $\theta_0 \in [0, 2\pi)$, where

$$m_0 = \frac{|\operatorname{Re}(\eta)|}{\sqrt{1 - \operatorname{Im}^2(\eta)}}, \quad (4.12)$$

$$\theta_0 = \begin{cases} \arcsin(-\operatorname{Im}(\eta)) & : \operatorname{Re}(\eta) \geq 0, \\ \pi - \arcsin(-\operatorname{Im}(\eta)) & : \operatorname{Re}(\eta) < 0. \end{cases} \quad (4.13)$$

Thus Lemma 6 immediately implies the conclusion by replacing η into $\eta = \eta(k)$. \square

We put $\theta_c(k)$ as $\arccos(\rho(k))$, that is,

$$\theta_c(k) = \arccos \left(\sqrt{\cos^2(\alpha - \beta) - \sin 2\alpha \sin 2\beta \cos^2 k} \right). \quad (4.14)$$

We can express explicitly B_u and $E_d \subset [0, 2\pi)^2$ as follows.

Theorem 2. *Let $\theta_0(k)$ and $\theta_c(k)$ be the above. Then we have*

$$B_u = \bigcup_{k \in [0, 2\pi)} [\theta_c(k), \pi - \theta_c(k)] \cup [\pi + \theta_c(k), 2\pi - \theta_c(k)] \quad (4.15)$$

$$E_d = \begin{cases} \{(k, \theta_0(k)) \mid k \in [0, 2\pi) \setminus \{\pi/2, 3\pi/2\}\} & : \sin(\alpha - \beta) \neq 0, \\ \emptyset & : \sin(\alpha - \beta) = 0, \end{cases} \quad (4.16)$$

We have the following property of B_u as a corollary.

Corollary 1. *There exists a wave number $k \in [0, 2\pi)$ at which the spectral gaps are closed if and only if “ $\sin(\alpha - \beta) = 0$ and $\sin 2\alpha \sin 2\beta \leq 0$ ” or “ $\sin(\alpha + \beta) = 0$ and $\sin 2\alpha \sin 2\beta > 0$ ”. In the first parameter class, the wave numbers are $k = \pi/2$ and $3\pi/2$, in the second parameter class, ones are $k = 0$ and π .*

We define $\theta_0(k)$ if the mass point $m_0(k)$ is strictly positive. Concerning the value of the mass point $m_0(k)$ described by (4.2), the parameter (α, β) must satisfy $\sin(\alpha + \beta) \neq 0$ and under this parameter, we set the domain of $\theta_0(k)$ as $[0, 2\pi) \setminus \{\pi/2, 3\pi/2\}$. Under this setting of the parameter and the domain, we call $\theta_0(k)$ the quasi-energy and its derivative group-velocity (of the edge state).

Corollary 2. *The quasi-energy is monotone on $\mathbb{T} := \mathbb{R}/(2\pi\mathbb{Z})$, and is discontinuous only at $k = \pi/2$ and $3\pi/2 \bmod(2\pi)$ on \mathbb{T} . At these points there is a jump, that is,*

$$\lim_{k \uparrow \pi/2} \theta_0(k) \neq \lim_{k \downarrow \pi/2} \theta_0(k), \quad \lim_{k \uparrow 3\pi/2} \theta_0(k) \neq \lim_{k \downarrow 3\pi/2} \theta_0(k).$$

More precisely, we divide the parameter $(\alpha, \beta) \in [0, 2\pi)^2$ into six classes up to the pair of signs; $(\operatorname{sgn}(\sin(\alpha + \beta)), \operatorname{sgn}(\sin(\alpha - \beta)))$, as follows:

(1) $(0, 0)$ and $(0, \pm)$ classes:

This is the condition closing the spectral gap at $k = 0$ and $k = \pi$. The edge state disappears for all $k \in [0, 2\pi)$, that is, $\theta_0(k)$ cannot be defined.

(2) $(+, +)$ class:

The quasi-energy is monotone increasing on \mathbb{T} . The discontinuous at $k = \pi/2$ occurs between “ $(\pi/2, \pi + \theta_c(\pi/2))$ and $(\pi/2, 2\pi - \theta_c(\pi/2))$ ” $\in [0, 2\pi)^2$ and the one at $k = 3\pi/2$ occurs between “ $(3\pi/2, \theta_c(3\pi/2))$ and $(\pi/2, \pi - \theta_c(3\pi/2))$ ” $\in [0, 2\pi)^2$, respectively.

(3) $(+, -)$ class:

The quasi-energy is monotone decreasing on \mathbb{T} . The discontinuous at $k = \pi/2$ occurs between “ $(\pi/2, \theta_c(\pi/2))$ and $(\pi/2, \pi - \theta_c(\pi/2))$ ” $\in [0, 2\pi)^2$ and the one at $k = 3\pi/2$ occurs between “ $(3\pi/2, \pi + \theta_c(3\pi/2))$ and $(\pi/2, 2\pi - \theta_c(3\pi/2))$ ” $\in [0, 2\pi)^2$, respectively.

(4) $(-, +)$ class:

The quasi-energy is monotone decreasing on \mathbb{T} . The discontinuous at $k = \pi/2$ occurs between “ $(\pi/2, \pi + \theta_c(\pi/2))$ and $(\pi/2, 2\pi - \theta_c(\pi/2))$ ” $\in [0, 2\pi)^2$ and the one at $k = 3\pi/2$ occurs between “ $(3\pi/2, \pi + \theta_c(3\pi/2))$ and $(\pi/2, 2\pi - \theta_c(3\pi/2))$ ” $\in [0, 2\pi)^2$, respectively.

(5) $(-, -)$ class:

The quasi-energy is monotone increasing on \mathbb{T} . The discontinuous at $k = \pi/2$ occurs between “ $(\pi/2, \theta_c(\pi/2))$ and $(\pi/2, \pi - \theta_c(\pi/2))$ ” $\in [0, 2\pi)^2$ and the one at $k = 3\pi/2$ occurs between “ $(3\pi/2, \pi + \theta_c(3\pi/2))$ and $(\pi/2, 2\pi - \theta_c(3\pi/2))$ ” $\in [0, 2\pi)^2$, respectively.

(6) $(\pm, 0)$ class:

This is the condition closing the spectral gap at $k = \pi/2$ and $k = 3\pi/2$. The group-velocity is zero, that is, we observe the flat band (dispersionless edge states).

By the above corollaries, the pattern shape of the dispersion relation $Bu \cup Ed$ is determined by the signs of $\sin 2\alpha \sin 2\beta = \sin^2(\alpha + \beta) - \sin^2(\alpha - \beta)$, $\sin(\alpha + \beta)$, $\sin(\alpha - \beta)$. See figure 3. We put the triple of the signs $(\epsilon_1, \epsilon_2, \epsilon_3)$, $(\epsilon_j \in \{\pm\})$. The first sign provides the shape of Bu : we have two bands which are symmetric with respect to $\theta = \pi$, and each band has period π ; if $\epsilon_1 = +$, then “peaks” appears at $k = \pi/2, 3\pi/2$ and “trough” at $k = 0, \pi$ while if $\epsilon_1 = -$, then we have the π -phase difference of the $\epsilon_1 = +$ case. If $\sin(\alpha + \beta) \neq 0$, the edge state appears as a bridge connecting the peaks (resp. troughs) of upper band and the one of the lower band for $\epsilon_1 = +$ case (resp. $\epsilon_1 = -$). The signs ϵ_2 and ϵ_3 describe the pattern shape of the edge state. If $\epsilon_2 = +$, then $\theta_0(0) = \pi$ and $\theta_0(\pi) = 0 (= 2\pi)$, while if $\epsilon_2 = -$, then we have the π -phase shift of $\epsilon_2 = +$ case. If $\epsilon_2\epsilon_3 = +$, then the group-velocity is positive, while if $\epsilon_2\epsilon_3 = -$, then the group-velocity is negative.

4.2 Topological phases

Here, we study symmetry and topological phases of the AE model. Since topological phases originate from bulk properties of the system, we focus on the system without boundaries. Thereby, we apply the time-evolution operator Γ in (2.13) for all the vertex set

$$V_0 = \mathbb{Z} \times \mathbb{Z} = \{(x, y) \mid x \in \mathbb{Z}, y \in \mathbb{Z}\},$$

in this section. In contrast to (3.2), applying the Fourier transform to the two-dimensional space of Γ , we derive the time-evolution operator in the wave number representation $\hat{\Gamma}_0(k_x, k_y) : \mathbb{C}^2 \rightarrow \mathbb{C}^2$ for fixed $(k_x, k_y) \in [0, 2\pi)^2$ described as

$$\hat{\Gamma}_0(k_x, k_y) = \hat{D}(k_x) H_\alpha \hat{D}(k_y) H_\beta. \quad (4.17)$$

We note that $\hat{D}(k)$ and H_γ can be written

$$\begin{aligned} \hat{D}(k) &= e^{-ik\sigma_3}, \\ H_\gamma &= e^{-i\gamma\sigma_2}, \end{aligned}$$

respectively, by using an identity matrix σ_0 and Pauli matrices σ_i ($i = 1, 2, 3$)

$$\sigma_0 = \begin{bmatrix} 1 & 0 \\ 0 & 1 \end{bmatrix}, \sigma_1 = \begin{bmatrix} 0 & 1 \\ 1 & 0 \end{bmatrix}, \sigma_2 = \begin{bmatrix} 0 & -i \\ i & 0 \end{bmatrix}, \sigma_3 = \begin{bmatrix} 1 & 0 \\ 0 & -1 \end{bmatrix}.$$

Firstly, we identify the presence or absence of three kinds of symmetry of the time-evolution operator $\hat{\Gamma}_0(k_x, k_y)$, which are relevant to topological phases, namely, time-reversal, particle-hole, and chiral symmetries. We see that $\hat{\Gamma}_0(k_x, k_y)$ retains particle-hole symmetry given by

$$\hat{P}\hat{\Gamma}_0(k_x, k_y)\hat{P}^{-1} = \hat{\Gamma}_0(-k_x, -k_y)$$

with the symmetry operator

$$\hat{P} = K,$$

where K stands for the complex conjugation. On the other hand, time-reversal and chiral symmetries

$$\begin{aligned} \hat{T}\hat{\Gamma}_0(k_x, k_y)\hat{T}^{-1} &= \hat{\Gamma}_0(-k_x, -k_y), \\ \hat{Y}\hat{\Gamma}_0(k_x, k_y)\hat{Y}^{-1} &= \hat{\Gamma}_0(k_x, k_y), \end{aligned}$$

respectively, are not generally satisfied even if we employ the symmetry-time frame method[3]. Therefore, the AE model belongs to the class D in the classification table of topological phases[25]. The topological numbers ν_{2d} for the AE model is derived in Ref. [4] from the so-called Rudner invariant[24]. The dependence on α and β of the topological number ν_{2d} is summarized in figure 2 (a). We note that the topological number ν_{2d} is finite except on lines in figure 2 (a), where spectrum gaps Bu are close and the topological number ν_{2d} is not well-defined. Along with the bulk-edge correspondence, we can predict the emergence of non-degenerated edge states in the AE model when the topological numbers ν_{2d} assigned by the parameter set (α, β) is non-zero since in the outer region from the cutting edge of the AE model the topological number ν_{2d} is zero. Taking into account the fact that topological number ν_{2d} is finite except closing of bulk spectra, the phase diagram seems to agree with Corollary 2 (1)-(5).

Corollary 2 (6), however, states that flat band spectrum appears nevertheless the spectrum gaps Bu are close and the topological number should be not well-defined. This disagreement can be resolved by introducing the topological number “in the one dimensional

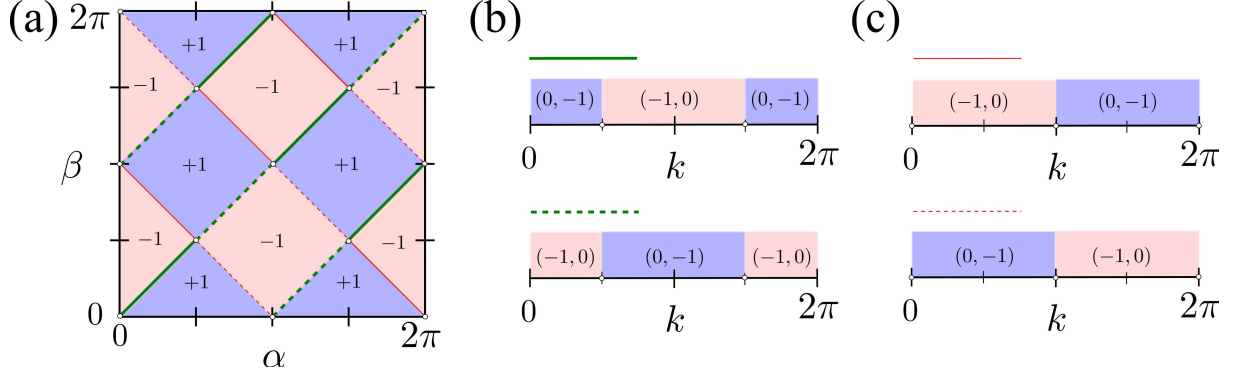


Figure 2: (a) The phase diagram of the topological number ν_{2d} derived in Ref. [4] as functions of α and β . In addition, the green thick and red thin (solid and dashed) lines represent the closing of bulk spectral gaps at the quasienergy 0 and π , where the topological numbers (ν_0, ν_π) are given in (4.24) and (4.28). (b) and (c) The wave number k dependence of the topological numbers (ν_0, ν_π) on the green thick and red thin (solid and dashed) lines, respectively. At the points shown by open circles in all figures, any topological numbers are not defined. Note that the topological numbers on the red thin lines cannot be applied to the AE model.

system”[26]. To this end, we put the condition for α and β to satisfy the case (6) of Corollary 2

$$\beta \in \{\alpha + n\pi \mid n \in \mathbb{Z}, \alpha \in [0, 2\pi) \setminus \{0, \frac{\pi}{2}, \pi, \frac{3\pi}{2}\}\}, \quad (4.18)$$

into (4.17). Then, the time-evolution operator becomes

$$\hat{\Gamma}_0(k_x, k_y; n, \alpha) = (-1)^n \hat{\Gamma}_0(k_x, k_y; \alpha), \quad \hat{\Gamma}_0(k_x, k_y; \alpha) = \hat{D}(k_x) H_\alpha \hat{D}(k_y) H_\alpha.$$

Since the prefactor $(-1)^n = e^{in\pi}$ only shifts the quasi-energy by $n\pi$, we can focus on $\hat{\Gamma}_0(k_x, k_y; \alpha)$ and recover the prefactor at the end of calculations. Now, by shifting the origin of time to derive a time-evolution operator fitted in the symmetry-time frame[3], we see the recovering chiral symmetry as

$$\begin{aligned} \hat{Y} \hat{\Gamma}'_0(k_x, k_y; \alpha) \hat{Y}^{-1} &= (\hat{\Gamma}'_0(k_x, k_y; \alpha))^{-1}, \\ \hat{\Gamma}'_0(k_x, k_y; \alpha) &= \hat{D}(k_x/2) H_\alpha \hat{D}(k_y) H_\alpha \hat{D}(k_x/2), \end{aligned} \quad (4.19)$$

with the chiral symmetry operator

$$\hat{Y} = \sigma_1. \quad (4.20)$$

Since $\hat{\Gamma}'_0(k_x, k_y; \alpha)$ also retains particle-hole symmetry, the system with parameters (4.18) belongs to the class BDI. While the class BDI in two dimensions does not have finite topological numbers, chiral symmetry classes are able to have an integer topological number in case of one dimension[25]. Therefore, we fix k_y of the time-evolution operator $\hat{\Gamma}'_0(k_x, k_y; \alpha)$ in (4.19) and regard it as a parameter $k \in [0, 2\pi)$. In the end, we consider the following time-evolution operator,

$$\hat{\Gamma}'_0(k_x; k, n) = (-1)^n \hat{\Gamma}'_0(k_x; k), \quad \hat{\Gamma}'_0(k_x; k) = \hat{D}(k_x/2) H_\alpha \hat{D}(k) H_\alpha \hat{D}(k_x/2). \quad (4.21)$$

Since k is fixed, $\hat{\Gamma}'_0(k_x; k)$ effectively describes the time-evolution in one dimension with chiral symmetry, while $\hat{D}(k)$ introduce a complex factor $e^{-ik\sigma_3}$. Therefore, the system belongs to the class AIII. Because of the presence of chiral symmetry, the topological number is calculated by the method in Ref. [3] as long as the bulk spectral gaps at k are open. In order to calculate the winding number, it is better to express $\hat{\Gamma}'_0(k_x; k)$ by using Pauli matrices as

$$\begin{aligned}\hat{\Gamma}'_0(k_x; k) &= d'_0(k_x)\sigma_0 + i \sum_{j=1,2,3} d'_j(k_x)\sigma_j, \\ d'_0(k_x) &= \cos k \cos(2\alpha) \cos k_x - \sin k \sin k_x, \\ d'_1(k_x) &= 0, \\ d'_2(k_x) &= d'_2 = -\sin(2\alpha) \cos k, \\ d'_3(k_x) &= -\sin k \cos k_x - \cos k \cos(2\alpha) \sin k_x.\end{aligned}$$

Furthermore, we apply a unitary transformation to $\hat{\Gamma}'_0(k_x; k)$ so that the chiral symmetry operator becomes $\hat{Y} = \sigma_3$,

$$\begin{aligned}\tilde{\Gamma}'_0(k_x; k) &= e^{-i\frac{\pi}{4}\sigma_2}\hat{\Gamma}'_0(k_x; k)e^{i\frac{\pi}{4}\sigma_2}, \\ &= d'_0(k_x)\sigma_0 + id'_3(k_x)\sigma_1 + id'_2(k_x)\sigma_2.\end{aligned}$$

The eigenvalue λ_{\pm} and corresponding eigenvectors $\psi'_{\pm}(k_x)$ of $\tilde{\Gamma}'_0(k_x; k)$ is given by

$$\begin{aligned}\lambda_{\pm} &= d'_0(k_x) \pm i\sqrt{1 - d_0'^2(k_x)}, \\ \psi'_{\pm}(k_x) &= \frac{1}{\sqrt{2}} \begin{bmatrix} \mp ie^{i\theta'(k_x)} \\ 1 \end{bmatrix}, \\ e^{i\theta'(k_x)} &= \frac{d'_2(k_x) + id'_3(k_x)}{\sqrt{1 - d_0'^2(k_x)}}\end{aligned}\tag{4.22}$$

Then, the winding number is given by

$$\begin{aligned}\nu' &= -\frac{i}{\pi} \int_0^{2\pi} \frac{1}{\psi'_{\pm}(k_x)} \frac{d\psi'_{\pm}(k_x)}{dk_x} dk_x \\ &= \frac{1}{2} \oint d\theta'(k_x).\end{aligned}$$

Therefore, the winding number is determined by whether $\theta'(k_x)$ in (4.22) makes a closed circle including the origin in the complex plane when k_x changes from 0 to 2π . Since $\sqrt{1 - d_0'^2(k_x)}$ is positive finite as long as the spectrum λ_{\pm} has a gap, we can focus on only the numerator in (4.22), $d'_2(k_x) + id'_3(k_x)$, in the following argument. Then, because $d'_2(k_x)$ is independent on k_x , $\theta'(k_x)$ does not make a circle and we have

$$\nu' = 0$$

for any α and k .

In order to calculate topological numbers ν_0 and ν_{π} for quasienergy 0 and π , respectively, we need to calculate the winding number for the other time-evolution operator $\hat{\Gamma}''_0(k_x; k)$ fitted in the different symmetry time frame

$$\hat{\Gamma}''_0(k_x; k) = \hat{D}(k/2)H_{\alpha}\hat{D}(k_x)H_{\alpha}\hat{D}(k/2).$$

Because of the relation $\hat{\Gamma}_0''(k_x; k) = \hat{\Gamma}_0'(k; k_x)$, the winding number ν'' of $\hat{\Gamma}_0''(k_x; k)$ is given by switching k_x and k of derivations of $\hat{\Gamma}_0'(k; k_x)$. In other words, the topological number ν'' is give by

$$\begin{aligned}\nu'' &= \frac{1}{2} \oint d\theta''(k_x), \\ e^{i\theta''(k_x)} &= \frac{d_2''(k_x) + i d_3''(k_x)}{\sqrt{1 - d_0''^2(k_x)}}, \\ d_2''(k_x) &= -\sin(2\alpha) \cos k_x, \\ d_3''(k_x) &= -\cos k \sin k_x - \sin k \cos(2\alpha) \cos k_x.\end{aligned}$$

Putting $u = d_2''(k_x)$ and $v = d_3''(k_x)$, we obtain the elliptic function of u and v

$$(\cos^2 k + \sin^2 k \cos^2(2\alpha))u^2 + \sin^2(2\alpha)v^2 - 2 \sin k \cos(2\alpha) \sin(2\alpha)uv = \cos^2 k \sin^2(2\alpha)$$

By properly rotating the coordinate, the above elliptic function is simply written down

$$\begin{aligned}u'^2 + \cos^2 k \sin^2(2\alpha)v'^2 &= \cos^2 k \sin^2(2\alpha), \\ \begin{bmatrix} u' \\ v' \end{bmatrix} &= \begin{bmatrix} \cos \eta & \sin \eta \\ -\sin \eta & \cos \eta \end{bmatrix} \begin{bmatrix} u \\ v \end{bmatrix}, \\ \cos \eta &= \frac{\cos(2\alpha)}{\Xi}, \quad \sin \eta = \frac{\sin k \sin(2\alpha)}{\Xi}, \quad \Xi = \sqrt{1 - \cos^2 k \sin^2(2\alpha)}.\end{aligned}\tag{4.23}$$

From (4.23), the winding number ν'' is determined as follows.

- (1) In the case of $\alpha = 0, \frac{\pi}{2}, \pi, \frac{3\pi}{2}$: (these values are excluded by (4.18))

Since (4.23) is reduced to $u' = u = 0$, the trajectory of $\theta''(k_x)$ becomes a line, and then $\nu'' = 0$.

- (2) In the case of $k = \frac{\pi}{2}, \frac{3\pi}{2}$:

Since (4.23) is reduced to $u' = \cos(2\alpha)u \pm \sin(2\alpha)v = 0$, the trajectory of $\theta''(k_x)$ becomes a line and then $\nu'' = 0$.

- (3) Otherwise:

The trajectory of $\mathbf{p} = (u(k_x), v(k_x))$ $k_x \in [0, 2\pi)$ is an ellipse with some rotation including the origin. The curvature of \mathbf{p} is expressed by

$$\kappa(k_x) = \frac{\dot{u}(k_x)\ddot{v}(k_x) - \ddot{u}(k_x)\dot{v}(k_x)}{(\dot{u}(k_x)^2 + \dot{v}(k_x)^2)^{3/2}}.$$

Here $\dot{w} = dw/dk_x$, and $\ddot{w} = d^2w/dk_x^2$, ($w = u, v$). The numerator of $\kappa(k_x)$ in this case can be computed as $\sin 2\alpha \cos k$. Thus the sign of κ coincides with one of $\sin 2\alpha \cos k$, which means $\nu'' \neq 0$ if and only if $\sin 2\alpha \cos k \neq 0$. Moreover since $\dot{u}(k_x) = \sin k_x \sin 2\alpha$, then $k_x = \pi$ is the unique point in $(0, 2\pi)$ so that the sign of $\dot{u}(k_x)$ is inverted, that is, for $\sin 2\alpha > 0$

$$\dot{u}(k_x) > 0 \quad (k_x \in (0, \pi)), \quad \dot{u}(k_x) < 0 \quad (k_x \in (\pi, 2\pi)),$$

and for $\sin 2\alpha < 0$, vice verse. Thus since the orbit is an ellipse with some rotation including the origin, we have $|\nu'| = 1$. Taking into account the prefactor $(-1)^n$ in (4.21), we can conclude that

$$\nu'' = \begin{cases} 1 & : (-1)^n \cos k \sin 2\alpha > 0, \\ -1 & : (-1)^n \cos k \sin 2\alpha < 0. \end{cases}$$

Finally, we use the formula to calculate topological numbers for zero and π energy states, ν_0 and ν_π , for one-dimensional quantum walks with chiral symmetry[3]

$$(\nu_0, \nu_\pi) = \left(\frac{\nu' + \nu'' - 1}{2}, \frac{\nu' - \nu'' - 1}{2} \right).$$

Putting ν' and ν'' into the above formula, we have

$$(\nu_0, \nu_\pi) = \begin{cases} (0, -1) & : (-1)^n \cos k \sin 2\alpha > 0, \\ (-1, 0) & : (-1)^n \cos k \sin 2\alpha < 0, \\ \text{undefined} & : \cos k \sin 2\alpha = 0. \end{cases} \quad (4.24)$$

The above result is summarized in figures 2(a) and (b). We remark that topological numbers ν_0 and ν_π depend on not only the angle of coin operators α (and n) but also the wave number k . Since the absolute value of both topological numbers is one, we predict a single edge states at quasi-energy 0 and π for each k by using the bulk-edge correspondence. Therefore, in the semi-infinite space V where k is continuous in $[0, 2\pi)$, the number of edge states at quasi-energy 0 and π becomes infinite as a consequence of the accumulation of topological numbers for each k . Then, infinitely degenerated edge states develop dispersionless flat bands at quasi-energy 0 and π , which is consistent with the proof of the case (6) in Corollary 2.

The above procedure is also applied to the case (1) in Corollary 2

$$\beta \in \{-\alpha + n\pi \mid n \in \mathbb{Z}, \alpha \in [0, 2\pi)\}, \quad (4.25)$$

where the bulk spectral gaps are close at $k = 0, \pi$ and there are no edge states. Putting (4.25) into (4.17) and regarding k_y as a fixed parameter $k \in [0, 2\pi)$, the time-evolution operator in the effective one dimension fitted in symmetry time frame is expressed as

$$\begin{aligned} \check{Y}\check{\Gamma}'_0(k_x; k)\check{Y}^{-1} &= (\check{\Gamma}'_0(k_x; k))^{-1}, \\ \check{\Gamma}'_0(k_x; k) &= \hat{D}(k_x/2)H_\alpha\hat{D}(k)H_{-\alpha}\hat{D}(k_x/2), \\ \check{\Gamma}'_0(k_x; k, n) &= (-1)^n\Gamma'_0(k_x; k) \end{aligned} \quad (4.26)$$

with the chiral symmetry operator

$$\check{Y} = \sigma_2. \quad (4.27)$$

More explicitly, $\check{\Gamma}'_0(k_x; k)$ is written down

$$\begin{aligned} \check{\Gamma}'_0(k_x; k) &= e'_0(k_x)\sigma_0 + i \sum_{j=1,2,3} e'_j(k_x)\sigma_j, \\ e'_0(k_x) &= \cos k \cos k_x - \sin k \cos(2\alpha) \sin k_x, \\ e'_1(k_x) &= -\sin k \sin(2\alpha), \\ e'_2(k_x) &= 0, \\ e'_3(k_x) &= -\cos k \sin k_x - \sin k \cos(2\alpha) \cos k_x. \end{aligned}$$

We remark that the chiral symmetry operators \check{Y} is different from \hat{Y} in (4.20). Applying the unitary transform $e^{i\frac{\pi}{4}\sigma_1}\tilde{\Gamma}'_0(k_x; k)e^{-i\frac{\pi}{4}\sigma_1}$, topological numbers for zero and π energy, ν_0 and ν_π , are derived in the same procedure as before. The result is summarized as

$$(\nu_0, \nu_\pi) = \begin{cases} (-1, 0) & : (-1)^n \sin k \sin 2\alpha > 0, \\ (0, -1) & : (-1)^n \sin k \sin 2\alpha < 0, \\ \text{undefined} & : \sin k \sin 2\alpha = 0. \end{cases} \quad (4.28)$$

We summarize the above result in figures 2 (a) and (c). We note, however, that the topological numbers in (4.28) cannot be applied to the AE model as explained below.

Remarkably, while we consider the case (1) in Corollary 2 which proofs the absence of edge states, topological numbers ν_0 and ν_π become finite except $\sin k \sin 2\alpha = 0$. However, when we predict the number of edge states by using the bulk-edge correspondence for the system with a boundary, we keep in mind that the boundary does not break symmetry retained in the bulk. Then, we check if the boundary realized by the shift operator in (2.10) [or (2.7)] retains chiral symmetry. Since we consider the shift operator in the position space in (2.10), we redefine chiral symmetry operators as,

$$\hat{Y} = \sum_{x,y} |x, y\rangle \langle x, y| \otimes \begin{bmatrix} \sigma_1 & 0 \\ 0 & \sigma_1 \end{bmatrix}, \quad \check{Y} = \sum_{x,y} |x, y\rangle \langle x, y| \otimes \begin{bmatrix} \sigma_2 & 0 \\ 0 & \sigma_2 \end{bmatrix}.$$

In order to retain chiral symmetry, the relation $XS''X^{-1} = S''^{-1}$ ($X \in \{\hat{Y}, \check{Y}\}$) should be satisfied. We can confirm that

$$\begin{aligned} \hat{Y}S''\hat{Y}S'' &= \sum_{x,y} |x, y\rangle \langle x, y| \otimes (|R\rangle\langle R| + |L\rangle\langle L| + |D\rangle\langle D| + |U\rangle\langle U|) \\ &= \sum_{x,y} |x, y\rangle \langle x, y| \otimes I_4 \quad : (x, y) \in V, \end{aligned}$$

where I_4 is an identity matrix of 4×4 matrices, while

$$\check{Y}S''\check{Y}S'' = \begin{cases} \sum_{x,y} |x, y\rangle \langle x, y| \otimes I_4 & : (x, y) \notin \partial D, \\ \sum_{x,y} |x, y\rangle \langle x, y| \otimes (-|R\rangle\langle R| + |L\rangle\langle L| + |D\rangle\langle D| + |U\rangle\langle U|) & : (x, y) \in \partial D. \end{cases}$$

Thereby, the boundary retains chiral symmetry given by \hat{Y} in (4.20), while it breaks chiral symmetry defined by the symmetry operator \check{Y} in (4.27). Therefore, the topological numbers in (4.28) cannot be applied to the AE model.

We note that a boundary realized by a shift operator with an extra phase i on the self loop

$$\begin{aligned} S''_i|x, y\rangle|J\rangle &= S'|x, y\rangle|J\rangle, \quad (J \in \{R, D, U\}), \\ S''_i|x, y\rangle|L\rangle &= \begin{cases} S'|x, y\rangle|L\rangle & : (x, y) \notin \partial D, \\ iS'|x, y\rangle|L\rangle & : (x, y) \in \partial D, \end{cases} \end{aligned}$$

satisfies $\check{Y}S''_i\check{Y}^{-1} = S''_i^{-1}$, but $\hat{Y}S''_i\hat{Y}^{-1} \neq S''_i^{-1}$. With the shift operator S''_i , we numerically confirmed that dispersionless edge states (flat bands) appear and agree with the topological numbers in (4.28) for parameters in the case (1) in Corollary 2, while there appear no edge states in the case (6).

4.3 Demonstrations

Here, we present plots of dispersion relations for bulk and edge states, which are written in Theorem 2, with specific values of α and β in figures 4-8 and compare them with the prediction by topological numbers. According to the bulk-edge correspondence, if topological numbers ν_{2d} , ν_0 , and ν_π are finite, we expect the presence of edge states. We can confirm that the dispersion relations for edge states agree well with the prediction from topological numbers.

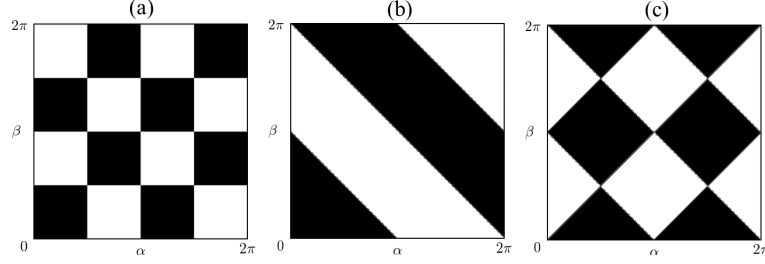


Figure 3: The black regions of $[0, 2\pi)^2$ depict (a) $\epsilon_1 = \sin 2\alpha \sin 2\beta > 0$ (b) $\epsilon_2 = \sin(\alpha + \beta) > 0$ (c) $\epsilon_2 \epsilon_3 = \sin(\alpha + \beta) \sin(\alpha - \beta) > 0$, respectively. On the lines $\alpha + \beta = \pi, 2\pi, 3\pi$ (see i.g., (b)), the edge state does not appear.

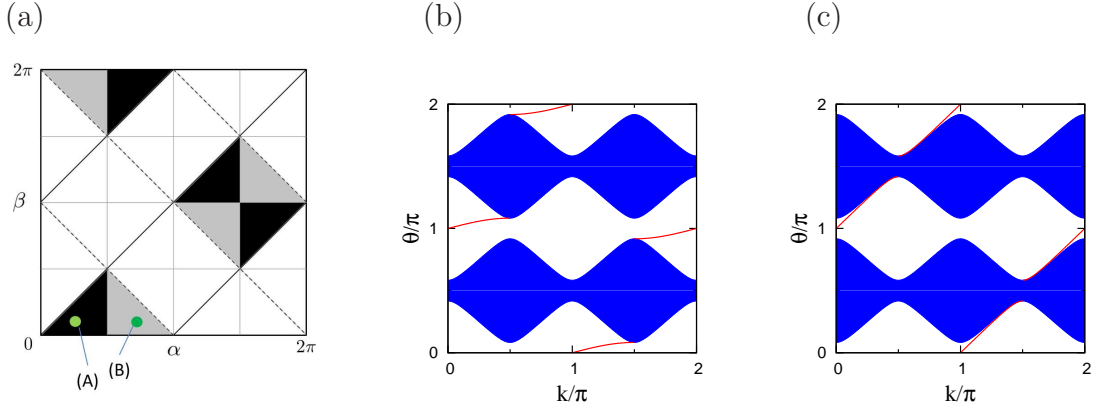


Figure 4: (a) The black and gray regions of the left figure are the parameter classes of $(+, +, +)$ and $(-, +, +)$, respectively. The topological number in these regions is $\nu_{2d} = +1$. (b) and (c) The dispersion relations for the parameter (A): $(\pi/4, \pi/6) \in (+, +, +)$ and (B): $(3\pi/4, \pi/6) \in (-, +, +)$, respectively. The blue region and red curves represent the bulk spectra and the quasi-energy for edge states, respectively.

5 Asymptotic behavior of quantum walk

We concentrate on the finding probability at the boundaries ∂D to find how the quantum walker recognizes the boundary: set $\nu_n : \mathbb{Z} \rightarrow [0, 1]$ as the probability that a quantum walker

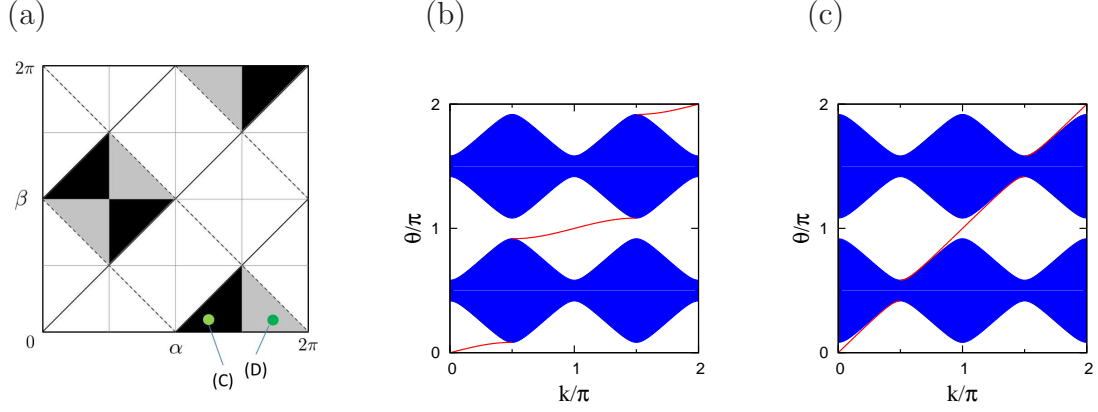


Figure 5: (a) The black and gray regions of the left figure are the parameter classes of $(+, -, -)$ and $(-, -, -)$, respectively. The topological number in these regions is $\nu_{2d} = +1$. (b) and (c) The dispersion relations for (C): $(5\pi/4, \pi/6) \in (+, -, -)$ and (D): $(7\pi/4, \pi/6) \in (-, -, -)$, respectively. The blue region and red curves represent the bulk spectra and the quasi-energy for edge states, respectively.

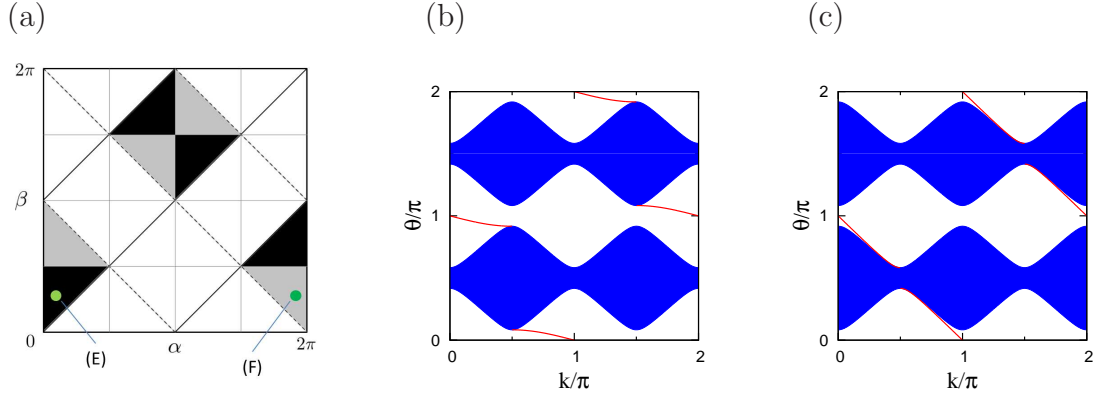


Figure 6: (a) The black and gray regions of the left figure are the parameter classes of $(+, +, -)$ and $(-, +, -)$, respectively. The topological number in these regions is $\nu_{2d} = -1$. (b) and (c) The dispersion relations for (E): $(\pi/6, \pi/4) \in (+, +, -)$ and (F): $(11\pi/6, \pi/4) \in (-, +, -)$, respectively. The blue region and red curves represent the bulk spectra and the quasi-energy for edge states, respectively.

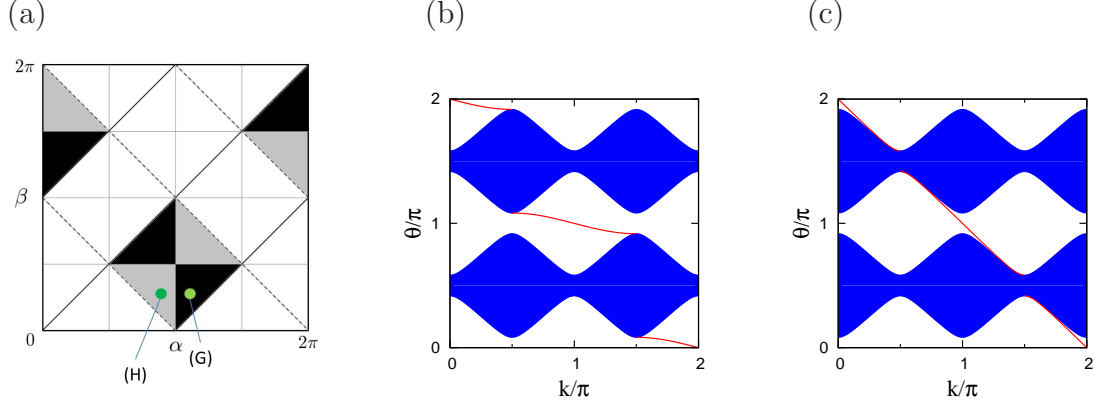


Figure 7: (a) The black and gray regions of the left figure are the parameter classes of $(+, -, +)$ and $(-, -, +)$, respectively. The topological number in these regions is $\nu_{2d} = -1$. (b) and (c) The dispersion relations for $G:(7\pi/6, \pi/4) \in (+, -, +)$ and $H):(5\pi/6, \pi/4) \in (-, -, +)$, respectively. The blue region and red curves represent the bulk spectra and the quasi-energy for edge states, respectively.

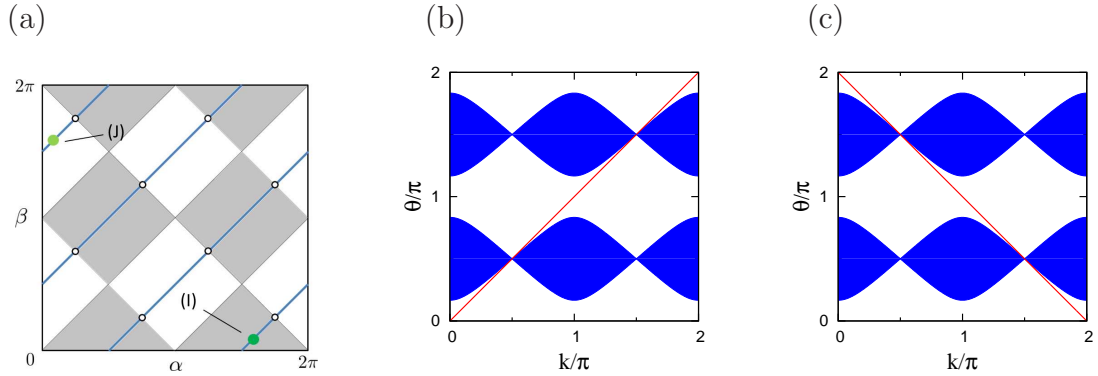


Figure 8: (a) The parameter (α, β) belongs to the blue real line in the left figure if and only if the edge state is described by straight lines, that is, the absolute-value of the group-velocity is 1. The topological number in gray and white regions is $\nu_{2d} = +1$ and -1 , respectively. (b) and (c) The dispersion relations for $(I):(5\pi/3, \pi/6) \in (-, -, -)$ and $(J):(\pi/6, 5\pi/3) \in (-, -, +)$, respectively. The blue region and red curves represent the bulk spectra and the quasi-energy for edge states, respectively.

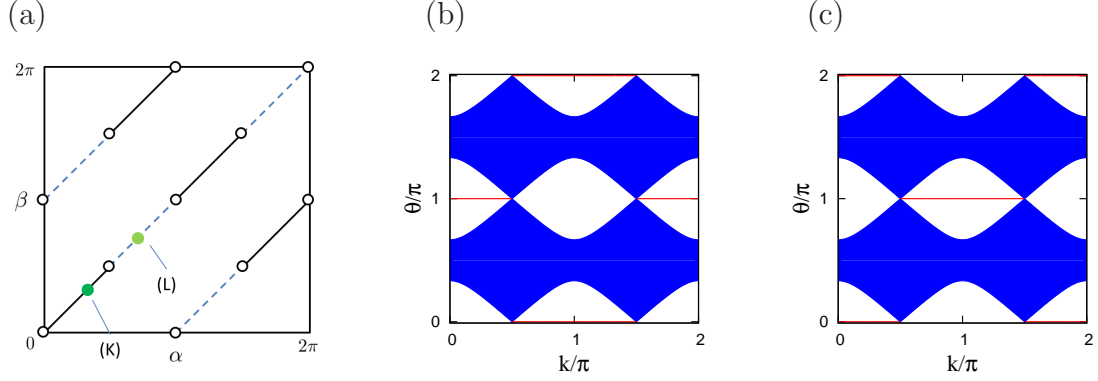


Figure 9: (a) The real lines depict the parameter classes of $(+, +, 0)$ where the topological numbers are given in figure 2(b). The dashed lines depict $(+, -, 0)$ where the topological numbers are given in figure 2(c). Remark that the classes $(-, \pm, 0)$ are empty. (b) and (c) The dispersion relations for (K): $(\pi/3, \pi/3) \in (+, +, 0)$ and (L): $(2\pi/3, 2\pi/3) \in (+, -, 0)$, respectively. The blue region and red curves represent the bulk spectra and the quasi-energy for edge states, respectively.

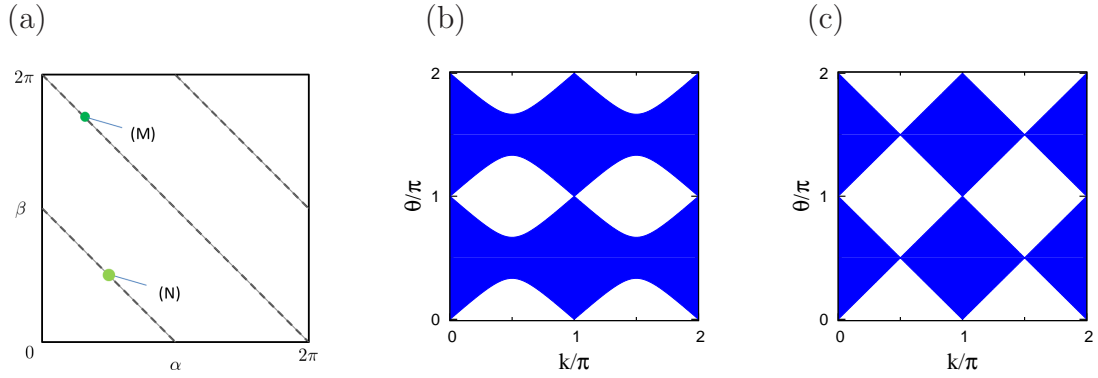


Figure 10: (a) The dashed lines depict the parameter classes of $(-, 0, 0)$ or $(-, 0, \pm)$. (b) and (c) The dispersion relations for (M): $(\pi/3, 5\pi/3) \in (-, 0, +)$ and (N): $(\pi/4, 3\pi/4) \in (-, 0, -)$, respectively. The blue region represents the bulk spectra.

is measured at time n at the boundary,

$$\nu_n(j) = |(U^n \psi_0)(a_j)|^2. \quad (5.1)$$

Here $a_j \in A$ is the self loop at $[0, j] \in V$. Recall that the initial state is fixed to the self loop at the origin $a_0 \in A$. We have

$$\hat{\psi}_n(k) := \sum_{j \in \mathbb{Z}} (U^{2n} \psi_0)(a_j) e^{ikj} = \hat{\varphi}_{n,1}(0; k).$$

Now we define some stochastic behavior at the boundary of the quantum walk as follows.

Definition 6.

- (1) We say linear spreading occurs at the boundary if and only if there exists a monotone non-decreasing function $F : \mathbb{R}_{\geq 0} \rightarrow [0, 1]$, which is not the identity function on $\mathbb{R}_{\geq 0}$, such that for any $y \in \mathbb{R}_{\geq 0}$,

$$\lim_{n \rightarrow \infty} \sum_{|j| < ny} \nu_n(j) = F(y).$$

In particular,

- (a) if $F(y)$ is continuous on $[0, 1]$, then we say continuously-linear spreading occurs;
- (b) if $F(y)$ is described by an indicator function $\mathbf{1}_{[c, \infty)}(y)$ ($c \in (0, 1]$), then we say ballistic spreading occurs.

- (2) We say localization occurs at the boundary if and only if there exists $j \in \mathbb{Z}$ such that

$$\limsup_{T \rightarrow \infty} \frac{1}{T} \sum_{n=0}^{T-1} \nu_n(j) > 0.$$

We have the following theorem:

Theorem 3. We put $s := \sin(\alpha + \beta) \neq 0$, and $r := \sin(\alpha - \beta)$.

- (1) If $0 < |r| < 1$, then the continuously linear spreading occurs: for any $a < b \in \mathbb{R}$,

$$\lim_{n \rightarrow \infty} \sum_{a \leq j/n \leq b} \nu_n(j) = \int_a^b g(y) dy \quad (5.2)$$

Here

$$g(y) = \frac{2s^2}{r^2} y^2 f_K(y; |r|) \times \begin{cases} \mathbf{1}_{[0, \infty)}(y) & : sr > 0, \\ \mathbf{1}_{(-\infty, 0]}(y) & : sr < 0, \end{cases} \quad (5.3)$$

where $f_K(x; |r|)$ is the Konno function with the parameter $|r|$.

- (2) If $|r| = 1$, then the ballistic spreading occurs:

$$\lim_{n \rightarrow \infty} \nu_n(\operatorname{sgn}(rs)(n - j)) = s^2 \delta_0(j). \quad (5.4)$$

(3) If $|r| = 0$, then localization occurs:

$$\lim_{n \rightarrow \infty} \nu_{2n}(j) = \begin{cases} \frac{s^2}{\pi^2} \frac{4}{(j^2-1)^2} & : j \text{ is even,} \\ 0 & : \text{otherwise.} \end{cases} \quad (5.5)$$

$$\lim_{n \rightarrow \infty} \nu_{2n+1}(j) = \begin{cases} \frac{s^2}{4} & : j \in \{\pm 1\}, \\ 0 & : \text{otherwise.} \end{cases} \quad (5.6)$$

The underlying dispersion relation classes of the limit theorem for the parameter (3) is $(\epsilon_1, \epsilon_2, 0)$, $(\epsilon_j \in \{\pm\} \ (j = 1, 2))$. In that dispersion relation, we have the flat edge state, that is $\theta_0(k)/dk = 0$ for all k . On the other hand, the one of the limit theorem for the parameter (2) is special class of $(-\epsilon_2, \epsilon_1)$, $(\epsilon_j \in \{\pm\} \ (j = 2, 3))$. In that dispersion relation, we have the linear edge state, that is, $|\theta_0(k)/dk| = 1$ for all k . The flatness and linearity of the edge state are reflected to the stochastic behaviors of the quantum walk on the boundary as localization and ballistic spreading, respectively.

Proof. The n -th iteration of the CMV matrix is expressed by a “quantum” version of the formula corresponding to the Karlin MacGregor’s formula for random walks:

$$(\mathcal{C}^n)_{i,j} = \int_{|z|=1} z^n \overline{\chi_i(z)} \chi_j(z) d\mu(z). \quad (5.7)$$

Concerning the one-to-one correspondence between canonical bases of \mathcal{C} and Type I quantum walk described by Lemma 4, $\mathcal{C}_{0,0}^n$ expresses the return complex valued amplitude to the origin at time n , that is,

$$\mathcal{C}_{0,0}^n = \hat{\psi}_n(k). \quad (5.8)$$

Combining (5.7) with (5.8) and Lemma 6, we have

$$\hat{\psi}_n(k) = \int_0^{2\pi} e^{in\theta} \left(\frac{w(\theta)}{2\pi} + m_0(k) \delta(\theta_0(k) - \theta) \right) d\theta. \quad (5.9)$$

The Riemann and Lebesgue lemma implies

$$\hat{\psi}_n(k) = e^{in\theta_0(k)} m_0(k) + o(1/\sqrt{n}). \quad (5.10)$$

We define the Fourier transform of ν_n by $\phi_n(\xi) := \sum_{j \in \mathbb{Z}} \nu_n(j) e^{i\xi j}$ ($\xi \in \mathbb{R}$). Here explicit expression for $\theta_0(k)$ and $m_0(k)$ are described by (4.2) and (4.3), respectively. Now we will proof our statement for each case.

Proof of part (1). It holds that

$$\phi_n(\xi) = \int_0^{2\pi} \overline{\hat{\psi}_n(k)} \hat{\psi}_n(k + \xi) \frac{dk}{2\pi}. \quad (5.11)$$

Under the assumption $\sin(\alpha - \beta) \sin(\alpha + \beta) \neq 0$, then using the expression (5.10), we obtain

$$\phi_n(\xi/n) = \int_0^{2\pi} e^{i\xi v(k)} m_0^2(k) \frac{dk}{2\pi} + o(1/\sqrt{n}), \quad (5.12)$$

where $v(k) = d\theta_0(k)/dk$:

$$\frac{d\theta_0}{dk} = \operatorname{sgn}(\sin(\alpha - \beta) \sin(\alpha + \beta)) |\sin(\alpha - \beta)| \frac{|\cos k|}{\sqrt{1 - \sin^2(\alpha - \beta) \sin^2 k}}. \quad (5.13)$$

Since

$$\frac{d}{dk} \left(\frac{\cos k}{\sqrt{1 - r^2 \sin^2 k}} \right) = - \frac{\sin k \cos^2(\alpha - \beta)}{(1 - \sin^2(\alpha - \beta) \sin^2 k)^{3/2}},$$

we have $0 \leq v(k) \leq |r|$ ($rs > 0$) and $-|r| \leq v(k) \leq 0$ ($rs < 0$). We consider $rs > 0$ case. For $0 \leq y \leq |r|$, due to the assumption $|r| < 1$, the solutions for $y = v(k)$ with respect to k are $k_1 < k_2 < k_3 < k_4$, which satisfy

$$\sin^2 k_j = \frac{r^2 - y^2}{r^2(1 - y^2)} \quad (j = 1, 2, 3, 4) \quad (5.14)$$

which implies $0 < k_1 < \pi/2 < k_2 < \pi < k_3 < 3\pi/2 < 2\pi$, and $k(y) := k_1$, $k_2 = \pi - k(y)$, $k_3 = \pi + k(y)$ and $k_4 = 2\pi - k(y)$. We divide the integration (5.12) into the four parts: $\int_0^{\pi/2} + \int_{\pi/2}^{\pi} + \int_{\pi}^{3\pi/2} + \int_{3\pi/2}^{2\pi}$. By taking $x = v(k)$ together with (5.14), we have

$$\frac{dv(k)}{dk} = - \frac{(1 - y^2) \sqrt{r^2 - y^2}}{\sqrt{1 - r^2}} = \frac{1}{\pi f_K(y; r)}. \quad (5.15)$$

and

$$m_0^2(k) = \frac{s^2}{r^2} y^2. \quad (5.16)$$

Then it holds

$$I_1(\xi) := \int_0^{\pi/2} e^{i\xi v(k)} m_0^2(k) \frac{dk}{2\pi} \quad (5.17)$$

$$= \int_0^{|r|} e^{i\xi y} \frac{s^2}{r^2} y^2 \frac{1}{2} f_K(y; r) dy. \quad (5.18)$$

In a similar fashion, we have $I_1(\xi) = I_2(\xi) = I_3(\xi) = I_4(\xi)$. Therefore we can rewrite (5.12) by

$$\phi(\xi) := \lim_{n \rightarrow \infty} \phi(\xi/n) = \int_0^{|r|} e^{i\xi y} \frac{s^2}{r^2} y^2 f_K(y; r) dy. \quad (5.19)$$

In the same way, for $rs < 0$ case we have

$$\lim_{n \rightarrow \infty} \phi(\xi/n) = \int_{-|r|}^0 e^{i\xi y} \frac{s^2}{r^2} y^2 f_K(y; r) dy. \quad (5.20)$$

Since $\phi(\xi)$ is continuous at $\xi = 0$, then the continuity theorem implies, for any $a < b \in \mathbb{R}$,

$$\lim_{n \rightarrow \infty} \sum_{a \leq j/n \leq b} \nu_n(j) = \int_a^b g(y) dy. \quad \square$$

Proof of part (2). Since $|r| = 1$, then $m_0(k)$ and $\theta_0(k)$ are reduced to $m_0(k) = |s|$, and

$$\theta_0(k) = \begin{cases} \pi + k & : (\operatorname{sgn}(s), \operatorname{sgn}(r)) = (+, +), \\ \pi - k & : (\operatorname{sgn}(s), \operatorname{sgn}(r)) = (+, -), \\ 2\pi - k & : (\operatorname{sgn}(s), \operatorname{sgn}(r)) = (-, -), \\ k & : (\operatorname{sgn}(s), \operatorname{sgn}(r)) = (-, +), \end{cases}$$

respectively. We set $\tau(j) := (U\psi_0)(a_j)$. Taking the inverse Fourier transform with inserting these values into $m_0(k)$ and $\theta_0(k)$ in (5.10), we have

$$\tau(n-j) := (U\psi)(a_{n-j}) \sim \int_0^{2\pi} e^{i(n-j)\theta_0(k)} m_0(k) e^{-i(n-j)k} \frac{dk}{2\pi} \quad (5.21)$$

$$= (-1)^n |s| \delta_0(j) \quad (5.22)$$

for $(\operatorname{sgn}(s), \operatorname{sgn}(r)) = (+, +)$ and $(-, -)$ cases. In the same way, we have $\tau(-n+j) \sim (-1)^n |s| \delta_0(j)$ for $(\operatorname{sgn}(s), \operatorname{sgn}(r)) = (+, -)$ and $(-, +)$ cases. \square

Proof of part (3). We put $B_1 = (-\pi/2, \pi/2) \bmod(2\pi)$, and $B_2 = (\pi/2, 3\pi/2)$. Since $r = 0$, $\theta_0(k)$ is flat, that is, by (4.3),

$$\theta_0(k) = \begin{cases} \pi & : k \in B_1 \\ 0 & : k \in B_2 \end{cases}$$

for $s > 0$, and

$$\theta_0(k) = \begin{cases} 0 & : k \in B_1 \\ \pi & : k \in B_2 \end{cases}$$

for $s < 0$. Moreover $m_0(k)$ is reduced to $|s| |\cos k|$. Then we have

$$\hat{\psi}_n(k) = |s| \times \begin{cases} (-1)^n |\cos k| & : k \in B_1 \\ |\cos k| & : k \in B_2 \end{cases} \quad (s > 0)$$

$$\hat{\psi}_n(k) = |s| \times \begin{cases} |\cos k| & : k \in B_1 \\ (-1)^n |\cos k| & : k \in B_2 \end{cases} \quad (s < 0)$$

For $s > 0$, taking the inverse Fourier transform to $\hat{\psi}_n(k)$, we have

$$\tau_n(j) \sim \int_0^{2\pi} \hat{\psi}_n(k) e^{-ikj} \frac{dk}{2\pi} \quad (5.23)$$

$$= |s| \left\{ (-1)^n \int_{k \in B_1} \cos k e^{-ikj} \frac{dk}{2\pi} + \int_{k \in B_2} |\cos k| e^{-ikj} \frac{dk}{2\pi} \right\} \quad (5.24)$$

We have

$$J_1(j) := \int_{k \in B_1} \cos k e^{-ikj} \frac{dk}{2\pi} = \begin{cases} \frac{(-1)^{j/2}}{\pi} \frac{1}{1-j^2} & : j \text{ is even,} \\ 1/4 & : j \in \{\pm 1\}, \\ 0 & : \text{otherwise;} \end{cases}$$

$$J_2(j) := \int_{k \in B_2} |\cos k| e^{-ikj} \frac{dk}{2\pi} = \begin{cases} \frac{(-1)^{j/2}}{\pi} \frac{1}{1-j^2} & : j \text{ is even,} \\ -1/4 & : j \in \{\pm 1\}, \\ 0 & : \text{otherwise.} \end{cases}$$

Then it holds

$$\tau_n(j) \sim |s|((-1)^n J_1(j) + J_2(j)) = \begin{cases} \frac{1+(-1)^n}{2} 2|s|(-1)^{j/2}/(\pi(1-j^2)) & : j \text{ is even,} \\ \frac{1+(-1)^{n-1}}{2} |s|/2 & : j \in \{\pm 1\}, \\ 0 & : \text{otherwise.} \end{cases}$$

In the same way for $s < 0$, we obtain the same expression for $\tau_n(j)$. Taking the square modulus to $\tau_n(j)$, we obtain the desired conclusion. \square

The group-velocity of the edge state is $v(k) = d\theta_0(k)/dk$, and the effective mass of the edge state is $M(k) = 1/(d^2\theta_0^2(k)/dk^2)$. The limit distribution provided by using the above physical quantities:

Corollary 3. *Let $v(k)$ and $M(k)$ be the above. For $0 < |\sin(\alpha + \beta)| < 1$, then*

$$\{(y, g(y)) : y \in \mathbb{R}\} = \{(v(k), 2m_0^2(k)M(k))/\pi : k \in [0, 2\pi)\}$$

Here $m_0(k)$ is the density of the edge state at $k \in [0, 2\pi)$ defined by (4.2).

We can obtain the distribution by the observation of the system and may be able to estimate the limit distribution $g(\cdot)$ from this data, which includes that we can also estimate its support length $|r|$ and the total contribution to the self loops $C_0 := \int_{-\infty}^{\infty} g(y)dy$. Under the setting that we have obtained the limit distribution $g(\cdot)$ or its estimation $\tilde{g}(\cdot)$, conversely we lead the following equation with respect to the group velocity $v(k) = d\theta_0(k)/dk$.

Corollary 4. *Let $g(\cdot)$, r and C_0 be the above. Then the group velocity $v(k)$ satisfies the following:*

$$g(v(k)) \frac{dv(k)}{dk} = \frac{2s^2/r^2}{\pi} v^2(k), \quad (5.25)$$

$$\int_0^{2\pi} |v(k)| \frac{dk}{2\pi} = \frac{2 \arcsin |r|}{\pi} \quad (5.26)$$

Here s^2 is expressed by

$$s^2 = \frac{r^2}{1 - \sqrt{1 - r^2}} C_0. \quad (5.27)$$

The second equation is a kind of boundary condition of the above differential equation. The above corollary suggests that we can estimate the underlying spectrum information of the quantum system from the observation information.

Proof. Since the second moment of $f_K(x; r)$ is $1 - \sqrt{1 - r^2}$ [17] and $f_K(x; |r|)$ is an even function, then the total contribution C_0 can be computed explicitly as (5.27). (5.25) directly comes from Corollary 3 and (5.16). Concerning the expression of $v(k)$ in (5.13), we divide the integration by four parts $\int_0^{\pi/2} + \int_{\pi/2}^{\pi} + \int_{\pi}^{3\pi/2} + \int_{3\pi/2}^{2\pi}$ so that $v(k)$ is a monotone function in each region. By (5.15),

$$\int_{m\pi/2}^{(m+1)\pi/2} |v(k)| \frac{dk}{2\pi} = \frac{1}{2} \int_0^{|r|} y f_K(y; r) dy, \quad (m = 0, 1, 2, 3).$$

RHS can be expressed by $\arcsin |r|/(2\pi)$. Then we have (5.26). \square

Concerning the explicit expression for $g(x)$ in (5.3), we also notice from this linear differential equation with respect to the group-velocity $v(k) = d\theta_0/dk$ that the group velocity of the edge state is expressed by an inverse of Konno's distribution $F_K(y; r) = \int^y f_K(x; r) dx$, that is,

$$v(k) = F_K^{-1}(2s^2 k/(r^2 \pi) + \zeta).$$

Here ζ satisfies

$$\int_0^{2\pi} |F_K^{-1}(2s^2 k/(r^2 \pi) + \zeta)| \frac{dk}{2\pi} = \frac{2 \arcsin |r|}{\pi}.$$

Before closing this section, we compare numerical results for the probability of the self loop at $[0, j]$ at the time step n , $\nu_n(j)$, with Theorem 3. In figures 11 and 12, we consider $0 < |r| < 1$ which gives continuously linear spreading behaviors. In the right figures of figures 11 and 12, we see that the scaled limit measure $g(y)/n$ in (5.3) runs through the “middle” of the oscillating $\nu_n(j)$. When we take the cumulation of $\nu_n(j)$ to ny , that is, $\sum_{j < ny} \nu_n(j)$, then in the left figures, we can see that the oscillation is almost wiped, and the cumulations of $\nu_n(j)$ and the integral of $g(y)$ are almost overlapped. This is the effect of the weakly convergence of Theorem 3.

Next, we consider the ballistic spreading with $|r| = 1$ and localization with $|r| = 0$ in figure 13. In this case, Theorem 3 and numerical results are almost consistent each other. We also confirm that the numerical result with $|r| = 0$ at odd-time steps completely agrees with (5.6).

Finally, applying Corollary 4, we derive the group velocity $v(k)$ from the numerical result $\nu_{400}(j)$ in figure 11, for example. To this end, we need to extract $g(v(k))$, r , and C_0 from $\nu_n(j)$. The parameter r is roughly estimated from figure 11 and C_0 is calculated from $C_0 = \sum_{j=0}^{400} \nu_{400}(j)$. To determine $g(v(k))$, we use the relation $y = j/n = v(k)$ and the fact that the cumulation of $\nu_n(y)$ shows less oscillations, which makes numerical fittings stable. Assuming that the integral of $g(y)$ is well approximated by a polynomial whose lowest order is third:

$$G(y) = \int_0^y g(y') dy' \approx \begin{cases} \sum_{m=3}^M g_m y^m & : 0 \leq y \leq r \\ C_0 & : y > r \end{cases} \quad (5.28)$$

we determine coefficient g_m up to the order $M = 5$ by numerically fitting to the cumulation of $\nu_n(j)$ as shown in figure 14(a). We summarize extracted values as follows:

$$g_3 = 52.47 \pm 5.64, \quad g_4 = -483.16 \pm 54.24, \quad g_5 = 1449.38 \pm 129.12, \quad r = 0.26, \quad C_0 = 0.47456.$$

From (5.25) and (5.28), we obtain

$$\sum_{m=3}^M \frac{m}{m-2} g_m y^{m-2} = \frac{2s^2/r^2}{\pi} (k - k_0), \quad (5.29)$$

where k_0 is a constant of integration. In the case of $M = 5$, one of the general solutions of $y = v(k)$ is guaranteed to be real. Then, we determine k_0 which satisfies (5.26). In figure 14(b), we compare the $|v(k)|$ obtained from the probability $n_{400}(j)$ with the exact solution in (5.13) and confirm that we can derive $|v(k)|$ from $\nu_n(j)$.

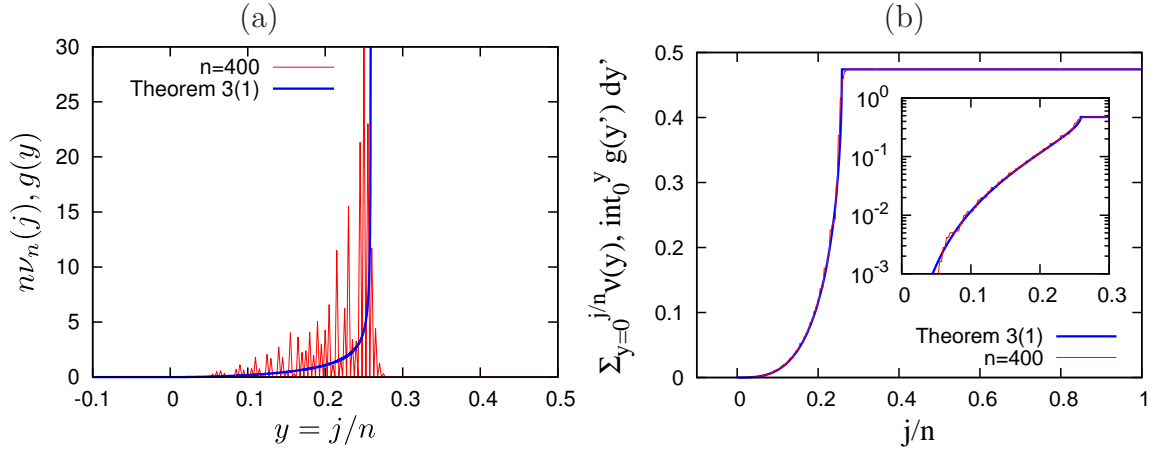


Figure 11: The rescaled measure on self loops $n\nu_n(j)$ at time steps $n = 400$ obtained by numerical simulations (a), and the distribution is obtained by (b) (red thin curves), in case of $(\alpha, \beta) = (\pi/4, \pi/6)$ whose dispersion relations are given in (b) in figure 4. The corresponding limit density $g(y)$ in (5.3) and distribution in (5.2) in Theorem 3 (1) is shown by blue thick curves. Inset of (b): the semi-log plot of the distribution

6 Limit distributions towards bulk

In the previous section, we showed limit theorems of the finding probability at the self loops on the boundary. In this section, we will show how the contribution of the edge states to the behavior of the quantum walk decays toward the bulk. To this end, we provide a limit theorem corresponding to Theorem 3 of the finding probability at the other arcs for $0 < |r| < 1$ and $s \neq 0$ case.

We put $\varphi'_n := \hat{\Gamma}_k^n \varphi'_0$ with $\varphi'_0(j) = \delta(j)^T [0, 1]$, where $\hat{\Gamma} : \ell^2(\mathbb{Z}_+; \mathbb{C}^2) \rightarrow \ell^2(\mathbb{Z}_+; \mathbb{C}^2)$ is defined in (3.2). Recall that we have shown that φ'_n , which is the n -th iteration of the quantum walk

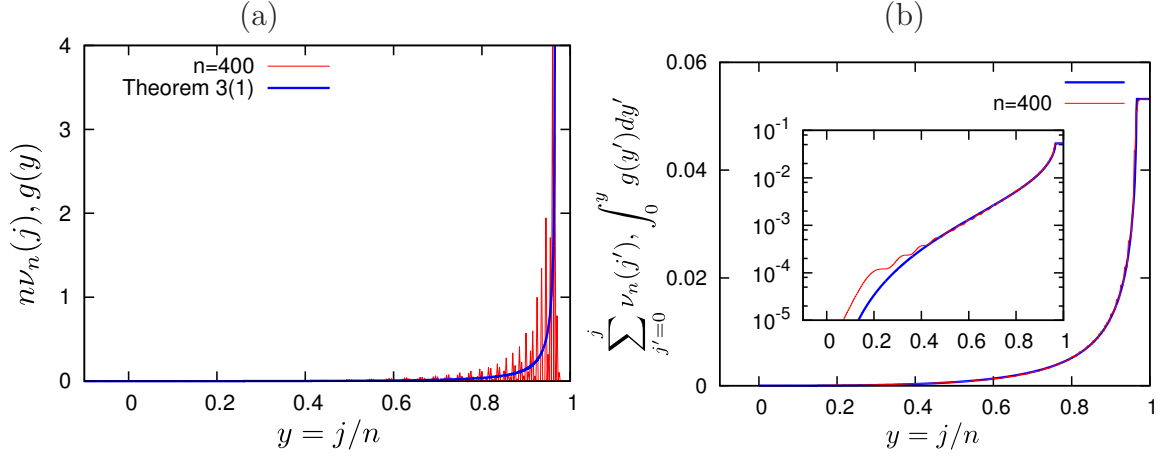


Figure 12: The rescaled measure on self loops $n\nu_n(j)$ at time steps $n = 400$ obtained by numerical simulations (a), and the distribution is obtained by (b) (red thin curves), in case of $(\alpha, \beta) = (3\pi/4, \pi/6)$ whose dispersion relations are given in (b) in figure 4. The corresponding limit density $g(y)$ in (5.3) and distribution in (5.2) in Theorem 3 (1) is shown by blue thick curves. Inset of (b): the semi-log plot of the distribution

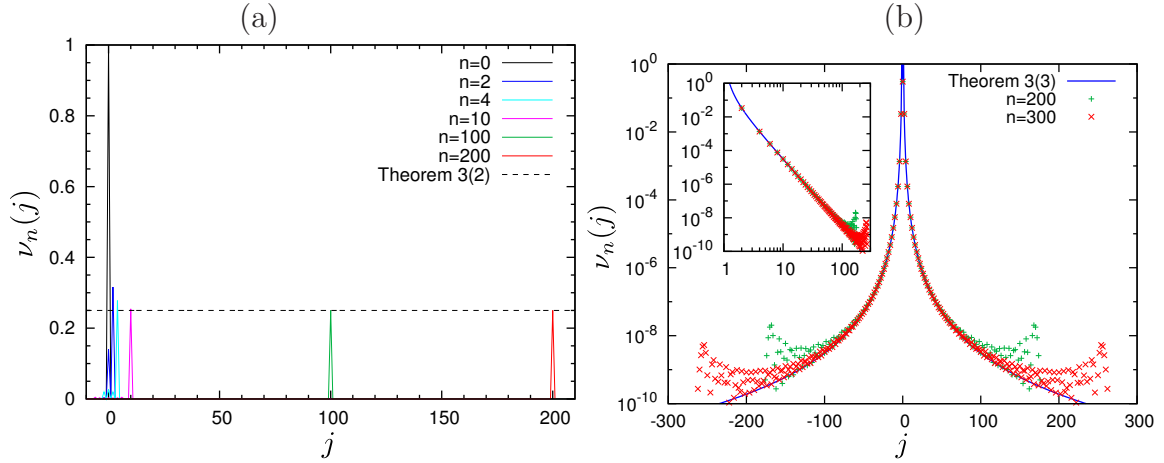


Figure 13: The measure on self loops $n\nu_n(j)$ at various time steps obtained by numerical simulations with (a) $(\alpha, \beta) = (5\pi/3, \pi/6)$ and (b) $(\pi/3, \pi/3)$ whose dispersion relations are given in (k) in figure 8 and (i) in figure 9, respectively. (a) The corresponding limit measures $\lim_{n \rightarrow \infty} \nu_n(j)$ in (5.4) in Theorem 3 (2) is shown by the dashed line. (b) The corresponding limit measures $\lim_{n \rightarrow \infty} \nu_n(j)$ in (5.5) in Theorem 3 (3) is shown by the blue thick curves. Inset: the log-log plot of the main figure.

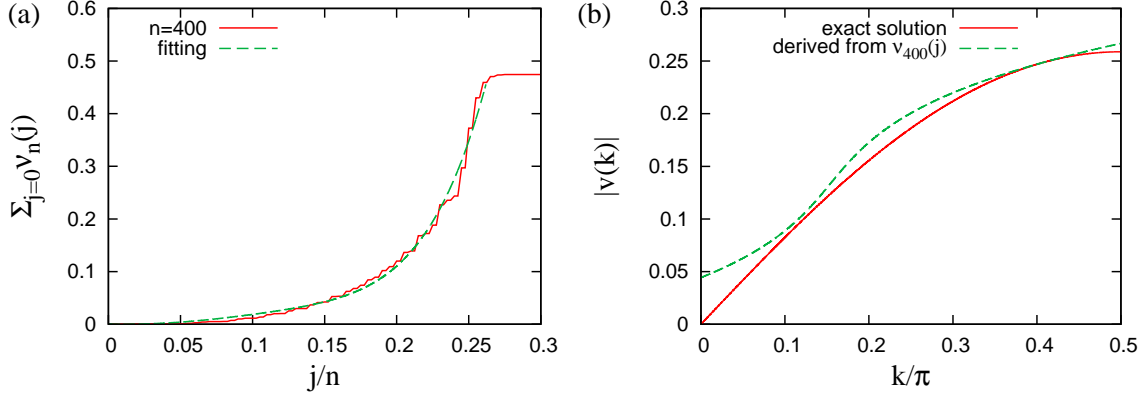


Figure 14: (a) The cumulation of $\nu_{400}(j)$ (red solid curve) in figure 11(a) and $G(y) = \sum_{m=3}^5 g_m y^m$ obtained by the numerical fitting (green dashed curve). (b) The group velocity $|v(k)|$ derived from $\nu_{400}(j)$ with $k_0 = -0.602$ (green dashed curve) and the exact solution in (5.13) (red solid curve).

on the Fourier space, is expressed by the n -th power of the CMV matrix \mathcal{C}_k in (3.12), that is,

$$\varphi'_n = \Lambda_k^{-1} \mathcal{C}_k^n \Lambda_k \varphi'_0.$$

We have

$$\begin{aligned} \varphi'_n(j) &= \begin{bmatrix} e^{-iw(2j+1)} (\mathcal{C}_k)_{0,2j+1} \\ e^{-iw(2j)} (\mathcal{C}_k)_{0,2j} \end{bmatrix} \\ &= \int_{|z|=1} z^n \begin{bmatrix} e^{-iw(2j+1)} x_{2j+1}(z) \\ e^{-iw(2j)} x_{2j}(z) \end{bmatrix} d\mu(z), \end{aligned} \quad (6.1)$$

where $x_j(z) = \overline{\chi_j(1/\bar{z})}$. The first equality derives from the definition of Λ_k with $(\Lambda_k \varphi'_0)(j) = \delta(j)$ and $({}^T \mathcal{C}_k)_{j,i} = (\mathcal{C}_k)_{i,j}$, the second equality is given by (5.7). This Lemma follows from [7, 19]:

Lemma 7. *Let \mathcal{C} be the CMV matrix with the Verblunsky parameter $(\gamma, 0, \gamma, 0, \dots)$. Assume $\text{Re}(\gamma) \neq 0$ which is a necessary and sufficient condition for $\sigma_p(\mathcal{C}) \neq \emptyset$. Then $\sigma_p(\mathcal{C}) = \{e^{i\beta}\}$ satisfying (4.13) and*

$$x_{2j}(e^{i\beta}) = \lambda^j, \quad x_{2j+1}(e^{i\beta}) = \lambda^{2j+1},$$

where

$$\lambda = \frac{\text{sgn}(\text{Re}(\gamma))}{\rho} \left(\sqrt{1 - \text{Im}^2(\gamma)} - |\text{Re}(\gamma)| \right).$$

Lemma 7 and the Riemann-Lebesgue lemma imply

$$\varphi'_n(j) = e^{in\theta_0(k)} m_0(k) \begin{bmatrix} e^{-iw(2j+1)} \lambda^{2j+1}(k) \\ e^{-iw(2j)} \lambda^{2j}(k) \end{bmatrix} + o(1/\sqrt{n}), \quad (6.2)$$

where

$$\lambda(k) = \frac{\text{sgn}(\text{Re}(\eta(k)))}{\rho(k)} \left(\sqrt{1 - \text{Im}^2(\eta(k))} - |\text{Re}(\eta(k))| \right).$$

Recall that $U : \mathcal{A} \rightarrow \mathcal{A}$ is the unitary time evolution of the quantum walk and $\psi_0 \in \mathcal{A}$ is the initial state. Also recall that the rebelling of each element of A in Definition 1. We put $\psi_n = U^{2n}\psi_0$. For $(j, m) \in V$ and $d \in \{0, 1\}$, the square modulus of $\psi_n((j, m); d)$ is the probability that we find the state $((j, m); d)$ after n -iteration of U starting from $((0, 0); 1)$. So we newly introduce the probability measure on $\nu_n : \mathbb{Z}_+ \times \mathbb{Z} \rightarrow [0, 1]$ such that

$$\nu_n(2j, m) := |\psi_n((j, m); 1)|^2 \quad \text{and} \quad \nu_n(2j+1, m) := |\psi_n((j, m); 0)|^2.$$

Remark that $\nu_n(0, m)$ is identical with $\nu_n(m)$ which was discussed in the previous section. We set the Fourier transform of them such that for $j \in \mathbb{Z}_+$, $n \in \mathbb{Z}_+$ and $\xi \in \mathbb{R}$,

$$\phi_n^{(j)}(\xi) = \sum_{m \in \mathbb{Z}} \nu_n(j, m) e^{i\xi m}.$$

Remark that $\phi_n(0, \xi)$ coincides with $\phi_n(\xi)$ in the previous section.

In the above discussion, we fixed k and treated $\hat{\varphi}_n$ as $\varphi'(\cdot) = \hat{\varphi}_n(\cdot; k) \in \ell^2(\mathbb{Z}_+; \mathbb{C}^2)$ while in the following, we will treat $\hat{\varphi}_n$ as the function of k for fixed j , that is, $\hat{\varphi}_n(j; \cdot) \in L^2([0, 2\pi]; \mathbb{C}^2)$. We put $\hat{\varphi}_n(j; k) := {}^T[\hat{\varphi}_{n,0}(j; k), \hat{\varphi}_{n,1}(j; k)]$. It is obtained that

$$\phi_n^{(2j)}(\xi) = \int_0^{2\pi} \overline{\hat{\varphi}_{n,1}(j; k)} \hat{\varphi}_{n,1}(j; k + \xi) \frac{dk}{2\pi}, \quad (6.3)$$

$$\phi_n^{(2j+1)}(\xi) = \int_0^{2\pi} \overline{\hat{\varphi}_{n,0}(j; k)} \hat{\varphi}_{n,0}(j; k + \xi) \frac{dk}{2\pi} \quad (6.4)$$

Since $r \neq 0$, replacing ξ into ξ/n in the above equation and using the expansion (6.2), we can obtain

$$\begin{bmatrix} \phi_n^{(2j+1)}(\xi/n) \\ \phi_n^{(2j)}(\xi/n) \end{bmatrix} = \int_0^{2\pi} e^{i\xi v(k)} m_0^2(k) \begin{bmatrix} \lambda^{2(j+1)}(k) \\ \lambda^{2j}(k) \end{bmatrix} \frac{dk}{2\pi} + o(1/\sqrt{n}). \quad (6.5)$$

Since $0 < |r| < 1$, then putting $y = v(k)$ for $k \in [0, 2\pi)$, we have

$$\lambda^2(k) = \frac{|r| - |s||y|}{|r| + |s||y|}.$$

Combining the above with (5.15) (5.16), we obtain

$$\lim_{n \rightarrow \infty} \phi_n^{(j)}(\xi/n) = \int_{-\infty}^{\infty} e^{i\xi y} g(j, y) dy.$$

Here the measure $g : \mathbb{Z}_+ \times \mathbb{R} \rightarrow \mathbb{R}_+$ is denoted by

$$g(2j+1, y) = \frac{s^2}{r^2} y^2 f_K(y; |r|) \zeta^{j+1}(y) \times \begin{cases} \mathbf{1}_{[0, \infty)}(y) & : sr > 0, \\ \mathbf{1}_{(-\infty, 0]}(y) & : sr < 0, \end{cases} \quad (6.6)$$

$$g(2j, y) = \frac{s^2}{r^2} y^2 f_K(y; |r|) \zeta^j(y) \times \begin{cases} \mathbf{1}_{[0, \infty)}(y) & : sr > 0, \\ \mathbf{1}_{(-\infty, 0]}(y) & : sr < 0, \end{cases}$$

with

$$\zeta(y) = \frac{|r| - |s||y|}{|r| + |s||y|}. \quad (6.7)$$

We summarize this section in the following theorem which is an extended result of Theorem 3 (1) to the other arcs since $g(0, y)$ coincides with $g(y)$ given by (5.3):

Theorem 4. *Let $\nu_n : \mathbb{Z}_+ \times \mathbb{Z} \rightarrow [0, 1]$ and $g : \mathbb{Z}_+ \times \mathbb{R} \rightarrow \mathbb{R}_+$ be the above. For $0 < |r| < 1$ with $s \neq 0$, we have*

$$\lim_{n \rightarrow \infty} \sum_{a < m/n < b} \nu_n(j, m) = \int_a^b g(j, y) dy \quad (j \in \mathbb{Z}_+)$$

Remark that the limit measure $g(j, \cdot)$ has the support $[0, |r|)$ or $(-|r|, 0]$. If we insert $y = \text{sgn}(rs)r$ into (6.7), then $\zeta(y) = (1 - |s|)/(1 + |s|)$ holds, which agrees with (B21) in [4]; this is the decay rate of the edge state wavefunctions towards the bulk for the zero quasi energy. The normalized position $y = \text{sgn}(rs)r$ coincides with the maximal absolute value of the group-velocity $v(k)$. In such wave number k , the effective mass $M(k)$, which is the inverse of the derivative of $v(k)$, takes infinity which implies that the value $g(j; y)$ also takes infinity, see Corollary 3.

Remark that LHS in Theorem 4 for $s = 0$ case, which is equivalent to the condition of lack of the edge state, becomes zero and also remark that the limit measure $g : \mathbb{Z}_+ \times \mathbb{R} \rightarrow \mathbb{R}_+$ is not a probability measure; we have focused on only the effect of the edge state to the finding probability without the consideration on one of the bulk state. Indeed, putting $\Omega := \mathbb{Z}_+ \times \mathbb{R}$, supposing $rs > 0$, we have

$$\begin{aligned} \int_{\omega \in \Omega} g(\omega) d\omega &= \int_{-\infty}^{\infty} \sum_{j=0}^{\infty} g(j; y) dy = \int_0^{|r|} \frac{1 + \zeta(y)}{1 - \zeta(y)} \frac{s^2}{r^2} y f_K(y; |r|) dy \\ &= \int_0^{|r|} \frac{|s|}{|r|} y f_K(y; |r|) dy \leq |s|/2 < 1. \end{aligned}$$

Considering the missing value at least $1 - |s|/2$ which is the contribution of the bulk state (see for a detailed expression (4.15) of the spectrum of bulk and its density (4.11)) is one of the interesting future's work.

Acknowledgments.

NK and ES were supported by and Japan-Korea Basic Scientific Cooperation Program “Non-commutative Stochastic Analysis; New Aspects of Quantum White Noise and Quantum Walk” (2015-2016), and NK and ES were also supported by the Grant-in-Aid for Scientific Research Challenging Exploratory Research (JSPS KAKENHI No. JP15K13443) and for Young Scientists (B) (JSPS KAKENHI No. JP16K17637), respectively. HO was supported by a Grant-in-Aid for Scientific Research on Innovative Areas “Topological Materials Science” (JSPS KAKENHI No. JP16H00975) and also JSPS KAKENHI (No. JP16K17760 and No. JP16K05466).

References

- [1] Ambainis A, Bach E, Nayak A, Vishwanath A and Watrous J 2001 One-dimensional quantum walks *Proc. 33rd Annual ACM Symp. Theory of Computing* 37-49
- [2] Asbóth J K 2012 Symmetries, topological phases, and bound states in the one-dimensional quantum walk *Phys. Rev. B* **86**, 195414
- [3] Asbóth J K and Obuse H 2013 Bulk-boundary correspondence for chiral symmetric quantum walks *Phys. Rev. B* **88**, 121406(R)
- [4] Asboth J K and Edge J M 2015 Edge-state-enhanced transport in a two-dimensional quantum walk *Phys. Rev. A* **91** 022324
- [5] Cantero M J, Moral L and Velázquez L 2003 Five-diagonal matrices and zeros of orthogonal polynomials on the unit circle *Linear Algebra and its Applications* **362** 29-56
- [6] Cantero M J, Moral L and Velázquez L 2005 Minimal representations of unitary operators and orthogonal polynomials on the unit circle *Linear Algebra and its Applications* **405** 40-65
- [7] Cantero M J, Grünbaum F A, Moral L and Velázquez L 2010 Matrix valued Szegő polynomials and quantum walks *Communications on Pure and Applied Mathematics* **63** 464-507
- [8] Cedzich C, Geib T, Grunbaum F A, Stahl C, Velazquez L, Werner A H, Werner R F 2016 The topological classification of one-dimensional symmetric quantum walks *Preprint* arXiv:1611.04439
- [9] Cedzich C, Grunbaum F A, Stahl C, Velazquez L, Werner A H, Werner R F 2016 Bulk-edge correspondence of one-dimensional quantum walks *Journal of Physics A: Mathematical and Theoretical* **49** 21
- [10] Endo T, Konno N, and Obuse H 2015 Relation between two-phase quantum walks and the topological invariant *Preprint* arXiv:1511.04230
- [11] Endo S, Endo T, Konno N, Segawa E, Takei M 2015 Limit theorems of a two-phase quantum walk with one defect *Quantum Information and Computation* **15** 1373-1396
- [12] Franco C Di, McGettrick M, Busch Th 2011 Mimicking the probability distribution of a two-dimensional Grover walk with a single-qubit coin *Phys. Rev. Lett.* **106** 080502
- [13] Franco C Di, McGettrick M, Machida T, Busch Th 2011 Alternate two-dimensional quantum walk with a single-qubit coin *Phys. Rev. A* **84** 042337
- [14] Gudder S 1988 *Quantum Probability* (Academic Press Inc., CA)
- [15] Kitagawa T, Rudner M S, Berg E, Demler E 2010 Exploring topological phases with quantum walks *Phys. Rev. A* **82** 033429
- [16] Kitagawa T 2012 Topological phenomena in quantum walks; elementary introduction to the physics of topological phases *Quantum Information Processing* **11** 1107-1148
- [17] Konno N 2002 Quantum random walks in one dimension *Quantum Inf. Proc.* **1** 345-354
- [18] Konno N 2005 A new type of limit theorems for the one-dimensional quantum random walk *J. Math. Soc. Jpn.* **57** 1179-1195

- [19] Konno N and Segawa E 2011 Localization of discrete time quantum walks on a half line via the CGMV method *Quantum Inf. Comput.* **11** 485–495
- [20] Manouchehri K and Wang J B 2014 *Physical Implementation of Quantum Walks* (Quantum Science and Technology, Springer)
- [21] Obuse H, Asbóth J K, Nishimura Y, and Kawakami N 2015 Unveiling hidden topological phases of a one-dimensional Hadamard quantum walk *Phys. Rev. B* **92** 045424
- [22] Obuse H and Kawakami N 2011 Topological phases and delocalization of quantum walks in random environments *Phys. Rev. B* **84** 195139
- [23] Portugal R 2013 *Quantum Walks and Search Algorithms* (Quantum Science and Technology, Springer)
- [24] Rudner M S, Lindner N H, Berg E, and Levin M 2013 Anomalous Edge States and the Bulk-Edge Correspondence for Periodically Driven Two-Dimensional Systems *Phys. Rev. X* **3** 031005
- [25] Schnyder A P, Ryu S, Furusaki A, and Ludwig A W W 2008 Classification of topological insulators and superconductors in three spatial dimensions *Phys. Rev. B* **78** 195125
- [26] Schnyder A P and Ryu S 2011 Topological phases and surface flat bands in superconductors without inversion symmetry *Phys. Rev. B* **84** 060504(R)

Appendix A

The density of the Konno distribution [17, 18] with the parameter $p \in (0, 1)$ is denoted by

$$f_K(x; p) = \frac{\sqrt{1 - p^2}}{\pi(1 - x^2)\sqrt{p^2 - x^2}} \mathbf{1}_{(-p, p)}(x). \quad (\text{A.1})$$